



## Article

# Efficient Approaches for Solving Systems of Nonlinear Time-Fractional Partial Differential Equations

Hegagi Mohamed Ali <sup>1,\*</sup> , Hijaz Ahmad <sup>2</sup> , Sameh Askar <sup>3</sup> and Ismail Gad Ameen <sup>4,\*</sup> <sup>1</sup> Department of Mathematics, Faculty of Science, Aswan University, Aswan 81528, Egypt<sup>2</sup> Section of Mathematics, International Telematic University Uninettuno, 00186 Roma, Italy; hijaz555@gmail.com<sup>3</sup> Department of Statistics and Operations Research, College of Science, King Saud University, P.O. Box 2455, Riyadh 11451, Saudi Arabia; saskar@ksu.edu.sa<sup>4</sup> Department of Mathematics, Faculty of Science, South Valley University, Qena 83523, Egypt

\* Correspondence: hegagi\_math@aswu.edu.eg (H.M.A.); ismailgad@svu.edu.eg (I.A.)

**Abstract:** In this work, we present a modified generalized Mittag–Leffler function method (MGMLFM) and Laplace Adomian decomposition method (LADM) to get an analytic-approximate solution for nonlinear systems of partial differential equations (PDEs) of fractional-order in the Caputo derivative. We apply the MGMLFM and LADM on systems of nonlinear time-fractional PDEs. Precisely, we consider some important fractional-order nonlinear systems, namely Broer–Kaup (BK) and Burgers, which have found major significance because they arise in many physical applications such as shock wave, wave processes, vorticity transport, dispersal in porous media, and hydrodynamic turbulence. The analysis of these methods is implemented on the BK, Burgers systems and solutions have been offered in a simple formula. We show our results in figures and tables to demonstrate the efficiency and reliability of the used methods. Furthermore, our outcome converges rapidly to the given exact solutions.



**Citation:** Ali, H.M.; Ahmad, H.; Askar, S.; Ameen, I. Efficient Approaches for Solving Systems of Nonlinear Time-Fractional Partial Differential Equations. *Fractal Fract.* **2022**, *6*, 32. <https://doi.org/10.3390/fractalfract6010032>

Academic Editor:  
Costas Psychalinos

Received: 15 November 2021

Accepted: 27 December 2021

Published: 10 January 2022

**Publisher's Note:** MDPI stays neutral with regard to jurisdictional claims in published maps and institutional affiliations.



**Copyright:** © 2022 by the authors. Licensee MDPI, Basel, Switzerland. This article is an open access article distributed under the terms and conditions of the Creative Commons Attribution (CC BY) license (<https://creativecommons.org/licenses/by/4.0/>).

**Keywords:** fractional partial differential equations; Laplace transform; Adomian decomposition method; Mittag–Leffler function; analytic-approximate solutions

## 1. Introduction

Mathematical models within fractional calculus (FC) have been widely used in various fields of natural science and engineering. In the last few decades, throughout much of the literature, we can find the concept of “memory” as the main advantage to process a system of fractional differential equations. This property has a significant impact on the behavior of the solutions for the considered models (see, e.g., [1,2]). The non-locality property of the fractional derivatives [3,4] that gives preference to utilizing FC, means calculating a time-fractional derivative of a function  $f(t)$  at some time  $t = t_1$  and requires all the previous history. This effect justifies the use of FC to better explain real-life models. In general, these models actually made more progress than those without the memory concept [5–7]. Recently, some authors have added a significant amount of research in the area of FC and its applications in various branches of engineering and natural science, such as electrodynamics [8], nano-technology [9], finance [10], mathematical biology [11,12], and control theory [13,14].

There are numerous phenomena in physics, biology, chemistry, engineering, finance, and other applied sciences that are represented by differential equations. In recent years, there have been a special interest in fractional partial differential equations (FPDEs), especially nonlinear ones, because of their influence in many applied sciences, such as diffusion of biological populations, fluid flow, electromagnetic waves, control theory of dynamical systems, and so on (see, e.g., [15–19] and the references therein). The majority of scientific problems in physics, engineering, and biological systems are nonlinear and their exact solutions are not easy to find. For example, physical problems are mostly modeled using

higher nonlinear FPDEs. In fact, it is challenging to find the exact solutions to such problems. Consequently, numerical and approximate techniques must be applied. Many useful approaches have been utilized to solve nonlinear and linear fractional differential equations (FDEs), such as the Adomian decomposition method (ADM) [20], variational iteration method (VIM) [21,22], homotopy analysis method (HAM) [23–26], homotopy perturbation method (HPM) [27–29].

The Mittag–Leffler function (MLF) has acquired major significance because its participation in solving numerous applications of FDEs. The generalized MLF method (GMLFM) is utilized to solve ordinary FDEs [30]. The GMLFM is applied to find analytical and approximate solutions for nonlinear systems that have applications such as the smoking model [31,32], Lorenz system [33], Riccati differential equations [34], and so on. The efficiency and eligibility of the GMLFM derive from the fact that its results converge promptly to the exact solution, and that it also provides solutions in simple and convenient procedures. Moreover, the GMLFM can be modified to solve FPDEs, where the MLF undetermined coefficient method contributes to solve the homogeneous FPDEs [35]. The modification of the GMLFM was applied to solve time-fractional Korteweg–de Vries (KdV) and Korteweg–de Vries–Burgers (KdVB) equations [36]. Furthermore, this modification has been used to illustrate the dynamics of predator–prey population as in [37].

The Adomian decomposition method (ADM) is an effective analytical method, that was first introduced by Adomian in the 1980s (see, e.g., [38,39]) to solve differential equations describing physical phenomena [40]. Furthermore, the ADM was developed by using Laplace transformation. Briefly, the LADM has been developed using the Laplace transform and ADM. Thus, we can say that the LADM demonstrates how the Laplace transform may be combined with the ADM to obtain an analytic approximate solution of nonlinear differential equations. Precisely, we used the LDAM because the calculations are easy to follow and understand. Additionally, the LADM is able to converge to the exact solutions faster than the ADM. For more advantages of the LADM over ADM and the comparison between them, see, e.g., [41]. Numerous phenomena that are described by PDE and FPDEs have been solved using the LADM, like Swift–Hohenberg (SH) equation [42], Keller–Segel equation [43], time-fractional model of Navier–Stokes equation [44], Fisher’s equation [45], fractional-order telegraph equations [46], and third-order dispersive FPDEs [47].

In this article, we intend to obtain the analytical solution of the following nonlinear fractional partial differential equations (NFPDEs):

- Broer–Kaup (BK) system [48] of fractional order  $0 < \alpha < 1$

$$\begin{cases} {}^C\mathcal{D}_t^\alpha U + UU_x + V_x = 0, \\ {}^C\mathcal{D}_t^\alpha V + U_x + (UV)_x + U_{xxx} = 0, \end{cases} \quad (1)$$

with the initial conditions (ICs)

$$U(x, 0) = 1 + 2\tanh(x) \quad V(x, 0) = 1 - 2\tanh^2(x). \quad (2)$$

- Burgers’ system [49] of fractional order  $0 < \alpha < 1$

$$\begin{cases} {}^C\mathcal{D}_t^\alpha U(x, t) = U_{xx} + 2UU_x - UV_x - VU_x, \\ {}^C\mathcal{D}_t^\alpha V(x, t) = V_{xx} + 2VV_x - UV_x - VU_x, \end{cases} \quad (3)$$

with the ICs

$$U(x, 0) = \sin(x), \quad V(x, 0) = \sin(x). \quad (4)$$

- Burgers’ system [49]:

$$\begin{cases} {}^C\mathcal{D}_t^\alpha U(x, y, t) = W_x V_y - W_y V_x - U, \\ {}^C\mathcal{D}_t^\alpha V(x, y, t) = V - U_y W_x - U_x W_y, \\ {}^C\mathcal{D}_t^\alpha W(x, y, t) = W - V_y U_x - V_x U_y, \end{cases} \tag{5}$$

with the ICs

$$U(x, y, 0) = e^{x+y}, \quad V(x, y, 0) = e^{x-y}, \quad W(x, y, 0) = e^{-x+y}. \tag{6}$$

The motivation of this study was to introduce two analytical techniques called MGMLFM and LADM to solve a full general NFPDE. In order to determine the efficacy and accuracy of the used methods, we applied them to solve the previous nonlinear systems of FPDEs and compared the obtained results with known exact solutions and solutions obtained by other methods. Precisely, to the best knowledge of the authors, analytical solutions of Broer–Kaup and Burgers’ systems of fractional orders by the proposed methods have not previously been reported in the literature, which strongly motivated this work.

The rest of this article is structured as: Section 2, we present some necessary concepts of FC, helping us to understand the main results in this article. In Section 3, we introduce the analysis of the proposed methods to solve a general system of FPDEs. Section 4 is devoted to applying the MGMLFM and LADM to the construction of approximate solutions of some illustrative examples of nonlinear systems of FPDEs. Moreover, we offer numerical simulations to compare our results with the exact solution, in order to prove the accuracy and efficacy of our methodology. Finally, our conclusion is presented in Section 5.

## 2. Preliminaries

In this section, we give a brief overview of the most important definitions and concepts related to this article (see, e.g., [50–52]).

**Definition 1.** The Riemann–Liouville fractional integral of order  $\alpha > 0$  of a function  $f(t)$ , can be defined as

$$\begin{aligned} \mathfrak{I}_t^\alpha f(t) &= \frac{1}{\Gamma(\alpha)} \int_0^t (t - \zeta)^{\alpha-1} f(\zeta) d\zeta, \quad t > 0, \\ \mathfrak{I}_t^0 f(t) &= f(t), \end{aligned}$$

where  $\Gamma(\cdot)$  is the Euler gamma function, defined as follows:

$$\Gamma(\xi) = \int_0^\infty t^{\xi-1} e^{-t} dt, \quad (Re(\xi) > 0).$$

**Definition 2.** The Caputo fractional partial derivative of a function  $f(x, t)$  of order  $\alpha$  is defined as

$${}^C\mathcal{D}_t^\alpha f(x, t) = \frac{1}{\Gamma(m - \alpha)} \int_0^t (t - \zeta)^{m-\alpha-1} \frac{\partial^m f(x, \zeta)}{\partial \zeta^m} d\zeta, \quad t > 0,$$

for  $m - 1 < \alpha \leq m, m \in \mathbb{N}$ . In particular, for  $0 < \alpha < 1$ , the Caputo fractional partial derivative becomes

$${}^C\mathcal{D}_t^\alpha f(x, t) = \frac{1}{\Gamma(1 - \alpha)} \int_0^t (t - \zeta)^{-\alpha} \frac{\partial f(x, \zeta)}{\partial \zeta} d\zeta, \quad t > 0.$$

**Theorem 1.** Let  $f(x, t)$  be a differentiable function in the interval  $[0, T]$ ,  $m - 1 < \alpha \leq m$ ,  $m \in \mathbb{N}$ . Then,

$$\begin{aligned} {}^C\mathcal{D}_t^\alpha \mathcal{I}_t^\alpha f(x, t) &= f(x, t), \\ \mathcal{I}_t^\alpha {}^C\mathcal{D}_t^\alpha f(x, t) &= f(x, t) - \sum_{k=0}^{m-1} \frac{\partial^k f(x, t)}{\partial t^k} \Big|_{t=0} \frac{t^k}{k!}. \end{aligned}$$

**Proposition 1.** For  $m - 1 < \alpha \leq m$ ,  $m \in \mathbb{N}$  and  $\beta > -1$ , we have:

$$\begin{aligned} {}^C\mathcal{D}_t^\alpha t^\beta &= \frac{\Gamma(\beta + 1)}{\Gamma(\beta - \alpha + 1)} t^{\beta - \alpha}, \\ \mathcal{I}_t^\alpha t^\beta &= \frac{\Gamma(\beta + 1)}{\Gamma(\beta + \alpha + 1)} t^{\beta + \alpha}. \end{aligned}$$

**Definition 3.** Let  $F(x, s)$  be the Laplace transform of the function  $f(x, t)$ . Then, the Laplace transform of the Caputo fractional partial derivative is given by [53]

$$\mathcal{L}\{{}^C\mathcal{D}_t^\alpha f(t), s\} = s^\alpha F(s) - \sum_{i=0}^{n-1} s^{\alpha-i-1} f^{(i)}(0), \quad (n - 1 < \alpha \leq n); \quad n \in \mathbb{N}.$$

**Definition 4.** The two-parameter MLF is defined by:

$$E_{\alpha, \beta}(x) = \sum_{n=0}^{\infty} \frac{x^n}{\Gamma(n\alpha + \beta)}, \quad \alpha, \beta > 0.$$

If  $\beta = 1$ , this function is denoted by  $E_\alpha(\cdot)$ , and if  $\alpha = \beta = 1$  this function represents  $e^x$ .

**Lemma 1.** The fractional derivative of the GMLF is given as:

$${}^C\mathcal{D}_t^\alpha E_\alpha(\lambda t^\alpha) = {}^C\mathcal{D}_t^\alpha \left( \sum_{n=0}^{\infty} \frac{\lambda^n t^{n\alpha}}{\Gamma(n\alpha + 1)} \right) = \sum_{n=1}^{\infty} \frac{\lambda^n t^{(n-1)\alpha}}{\Gamma((n-1)\alpha + 1)} = \sum_{n=0}^{\infty} \frac{\lambda^{n+1} t^{n\alpha}}{\Gamma(n\alpha + 1)} = \lambda E_\alpha(\lambda t^\alpha).$$

**Theorem 2.** Assume that a nonlinear function  $N(u)$  and  $u = \sum_{l=0}^{\infty} \zeta^l u_l$ , then (see, e.g., [54])

$$\frac{\partial^n}{\partial \zeta^n} N(u)_{\zeta=0} = \frac{\partial^n}{\partial \zeta^n} N \left( \sum_{l=0}^{\infty} \zeta^l u_l \right)_{\zeta=0} = \frac{\partial^n}{\partial \zeta^n} N \left( \sum_{l=0}^n \zeta^l u_l \right)_{\zeta=0}.$$

### 3. Idea of the Used Methods

In this section, we introduce the idea behind the analysis of the proposed methods and how these methods were implemented to solve a general form of NFPDEs. For more details on the convergence analysis of these methods, we encourage the reader to consult [30–33,55].

#### 3.1. Analysis of the MGMLFM

In this subsection, we discuss the methodology of the MGMLFM to solve a general FPDEs. To this end, we consider a system of fractional-order nonlinear PDEs of the following general form

$${}^C\mathcal{D}_t^\alpha \mathbf{u}(\xi, t) = L(\mathbf{u}(\xi, t)) + N(\mathbf{u}(\xi, t)), \quad (7)$$

with the ICs

$$\mathbf{u}(\xi, 0) = \phi(\xi), \quad (8)$$

where  ${}^C\mathcal{D}_t^\alpha \mathbf{u}(\xi, t)$  is the Caputo fractional derivative of order  $p - 1 < \alpha \leq p$  for the function  $\mathbf{u}(\xi, t)$ , such that  $\mathbf{u} = (u_1, u_2, \dots, u_m)^T$ ,  $\Phi = (\phi_1, \phi_2, \dots, \phi_m)^T$  and  $\xi = (\xi_1, \xi_2, \dots, \xi_n) \in \mathbb{R}^n$ ,  $p, m, n \in \mathbb{N}$ . The nonlinear and linear operator of the function  $\mathbf{u}(\xi, t)$  are represented by  $L$  and  $N$ , respectively.

The MGMLFM assumes that the solution of  $\mathbf{u}(\xi, t)$  in Equation (7) can be written as an infinite series as follows:

$$\begin{aligned} u_1(\xi, t) &= w_1(\xi)E_\alpha(A_1 t^\alpha) = \sum_{j=0}^\infty w_1(\xi)A_1^j \frac{t^{j\alpha}}{\Gamma(j\alpha + 1)}, \\ u_2(\xi, t) &= w_2(\xi)E_\alpha(A_2 t^\alpha) = \sum_{j=0}^\infty w_2(\xi)A_2^j \frac{t^{j\alpha}}{\Gamma(j\alpha + 1)}, \\ &\vdots \\ u_m(\xi, t) &= w_m(\xi)E_\alpha(A_m t^\alpha) = \sum_{j=0}^\infty w_m(\xi)A_m^j \frac{t^{j\alpha}}{\Gamma(j\alpha + 1)}, \end{aligned} \tag{9}$$

where  $A_1, A_2, \dots, A_m$  are undetermined coefficients and  $w_1(\xi), w_2(\xi), \dots, w_m(\xi)$  are functions of the variable  $\xi$ . By using ICs (8), we have

$$w_1(\xi) = \phi_1(\xi), w_2(\xi) = \phi_2(\xi), \dots, w_m(\xi) = \phi_m(\xi).$$

Following to Lemma 1, Equations (9), (7) and ICs (8), we get:

$$\sum_{j=0}^\infty \phi_m(\xi)A_m^{j+1} \frac{t^{j\alpha}}{\Gamma(j\alpha + 1)} = L\left(\sum_{j=0}^\infty \phi_m(\xi)A_m^j \frac{t^{j\alpha}}{\Gamma(j\alpha + 1)}\right) + N\left(\sum_{j=0}^\infty \phi_m(\xi)A_m^j \frac{t^{j\alpha}}{\Gamma(j\alpha + 1)}\right), \quad m = 1, 2, \dots \tag{10}$$

Therefore, the linear term can be decomposed as

$$\begin{aligned} L(\mathbf{u}(\xi, t)) &= L\left(\sum_{j=0}^\infty \phi_m(\xi)A_m^j \frac{t^{j\alpha}}{\Gamma(j\alpha + 1)}\right) = L(\phi_m(\xi)) \sum_{j=0}^\infty A_m^j \frac{t^{j\alpha}}{\Gamma(j\alpha + 1)} \\ &= \lambda_m^* \phi_m(\xi) \sum_{j=0}^\infty A_m^j \frac{t^{j\alpha}}{\Gamma(j\alpha + 1)}, \end{aligned} \tag{11}$$

where  $\lambda_m^*$  is a constant. From He’s polynomials [54,56,57] and Theorem 2, the  $N(\mathbf{u}(\xi, t))$  can be decomposed as:

$$N(\mathbf{u}(\xi, t)) = N\left(\sum_{j=0}^\infty \phi_m(\xi)A_m^j \frac{t^{j\alpha}}{\Gamma(j\alpha + 1)}\right) = N(\phi_m(\xi))N\left(\sum_{j=0}^m u_j(\xi, t)\right). \tag{12}$$

Substituting Equations (11) and (12) into Equation (10), we can specify the recurrence relation (RR) and obtain the  $A_m$ , therefore we can get the solution of the NFPDEs.

### 3.2. LADM for System of FDEs

Here, we explain the basic idea of the LADM for solving Equations (7) and (8). By applying the Laplace transform to both sides of Equation (7) and using the linear property of this transformation, the result is

$$\mathcal{L}[{}^C\mathcal{D}_t^\alpha \mathbf{u}(\xi, t)] = \mathcal{L}[L(\mathbf{u}(\xi, t))] + \mathcal{L}[N(\mathbf{u}(\xi, t))].$$

Using Definition 3 and applying the formulas of the Laplace transform, we get:

$$s^\alpha \mathcal{L}[\mathbf{u}(\xi, t)] = s^{\alpha-1} \mathbf{u}(\xi, 0) + \mathcal{L}[L(\mathbf{u}(\xi, t))] + \mathcal{L}[N(\mathbf{u}(\xi, t))],$$

$$\mathcal{L}[\mathbf{u}(\xi, t)] = \frac{\phi(\xi)}{s} + \frac{1}{s^\alpha} \left( \mathcal{L}[L(\mathbf{u}(\xi, t))] + \mathcal{L}[N(\mathbf{u}(\xi, t))] \right). \quad (13)$$

The LADM represents the solution as an infinite series

$$\mathbf{u}(\xi, t) = \sum_{r=0}^{\infty} \mathbf{u}_r(\xi, t), \quad (14)$$

and the nonlinear terms in Equation (7) decompose as

$$N(\mathbf{u}(\xi, t)) = \sum_{r=0}^{\infty} \mathbf{A}_r, \quad (15)$$

where  $\mathbf{A}_r$  are Adomian polynomials and they can be calculated by the following formula:

$$\mathbf{A}_r = \frac{1}{r!} \frac{d^r}{d\lambda^r} \left[ N \sum_{i=0}^{\infty} (\lambda^i \mathbf{u}_i) \right] \Big|_{\lambda=0}, \quad r = 0, 1, 2, \dots \quad (16)$$

Substituting Equations (14) and (15) in Equation (16), we have:

$$\mathcal{L} \left[ \sum_{r=0}^{\infty} \mathbf{u}_r(\xi, t) \right] = \frac{\phi(\xi)}{s} + \frac{1}{s^\alpha} \left( \mathcal{L} \left[ L \left( \sum_{r=0}^{\infty} \mathbf{u}_r(\xi, t) \right) \right] + \mathcal{L} \left[ \sum_{r=0}^{\infty} \mathbf{A}_r \right] \right).$$

Then, we can write:

$$\begin{aligned} \mathcal{L}[\mathbf{u}_0(\xi, t)] &= \frac{\phi(\xi)}{s}, \\ &\vdots \\ \mathcal{L}[\mathbf{u}_r(\xi, t)] &= \frac{1}{s^\alpha} \left( \mathcal{L}[L(\mathbf{u}_{r-1}(\xi, t))] + \mathcal{L}[\mathbf{A}_{r-1}] \right), \quad r \geq 1. \end{aligned} \quad (17)$$

Then, applying the inverse Laplace transform to Equation (17), we obtain the values  $\mathbf{u}_r(\xi, t)$  recursively.

#### 4. Applications and Results

Here, we apply the MGMLFM and LADM on Equations (1), (3), and (5) and provide a comparison of the obtained results with the given exact solutions to present the accuracy and advantages of the used approaches.

**Example 1.** Let the system of NFPDEs (1) subject to ICs (2) and the known exact solutions of this system when  $\alpha = 1$  are given as [48]:

$$U(x, t) = 1 - 2 \tanh(t - x) \quad V(x, t) = 1 - 2 \tanh^2(t - x). \quad (18)$$

- Applying the MGMLFM, as the suggestions in equation (9). Let

$$U(x, t) = \sum_{n=0}^{\infty} F_1(x) A^n \frac{t^{n\alpha}}{\Gamma(n\alpha + 1)}, \quad (19)$$

$$V(x, t) = \sum_{n=0}^{\infty} F_2(x) B^n \frac{t^{n\alpha}}{\Gamma(n\alpha + 1)}, \quad (20)$$

where  $A, B$  are coefficients. From ICs (2), we have  $F_1(x) = U_0 = 1 + 2\tanh(x)$  and  $F_2(x) = V_0 = 1 - 2\tanh^2(x)$ . By using Equation (11), we write the linear term of (1) as follows:

$$L(U) = -\frac{\partial(1 - 2\tanh^2(x))}{\partial x} = 4\operatorname{sech}^2(x)\tanh(x),$$

$$L(V) = -\frac{\partial(1 + 2\tanh(x))}{\partial x} - \frac{\partial^3(1 + 2\tanh(x))}{\partial x^3} = 2\operatorname{sech}^2(x)(1 - 6\tanh^2(x)).$$

Similarly, the nonlinear term of Equation (1) is given as

$$N(U) = -(1 + 2\tanh(x))\frac{\partial(1 + 2\tanh(x))}{\partial x} = -2\operatorname{sech}^2(x)(1 + 2\tanh(x)),$$

$$N(V) = -(1 + 2\tanh(x))\frac{\partial(1 - 2\tanh^2(x))}{\partial x} - (1 - 2\tanh^2(x))\frac{\partial(1 + 2\tanh(x))}{\partial x}$$

$$= 2\operatorname{sech}^2(x)(-1 + 2\tanh(x) + 6\tanh^2(x)).$$

By using Equations (1) and (10), we get

$$\sum_{n=0}^{\infty} (U_0 A^{n+1} - 2\operatorname{sech}^2(x)(2\tanh(x)B^n - (1 + 2\tanh(x))C^n\Gamma(n\alpha + 1)))\frac{t^{n\alpha}}{\Gamma(n\alpha + 1)} = 0,$$

$$\sum_{n=0}^{\infty} (V_0 B^{n+1} - 2\operatorname{sech}^2(x)((1 - 6\tanh^2(x))A^n + (-1 + 2\tanh(x) + 6\tanh^2(x))C_*^n\Gamma(n\alpha + 1)))\frac{t^{n\alpha}}{\Gamma(n\alpha + 1)} = 0,$$

where

$$C^n = \sum_{k=0}^n \frac{A^k A^{n-k}}{\Gamma(k\alpha + 1)\Gamma((n-k)\alpha + 1)} \quad \text{and} \quad C_*^n = \sum_{k=0}^n \frac{A^k B^{n-k}}{\Gamma(k\alpha + 1)\Gamma((n-k)\alpha + 1)}.$$

Then, the RR are given by

$$A^{n+1} = \frac{2\operatorname{sech}^2(x)}{U_0} (2\tanh(x)B^n - (1 + 2\tanh(x))C^n\Gamma(n\alpha + 1)), \tag{21}$$

$$B^{n+1} = \frac{2\operatorname{sech}^2(x)}{V_0} ((1 - 6\tanh^2(x))A^n + (-1 + 2\tanh(x) + 6\tanh^2(x))C_*^n\Gamma(n\alpha + 1)).$$

Substituting the values of  $n$  and doing some computation, we obtain the following:

$$A^0 = 1, \quad B^0 = 1,$$

$$A^1 = -\frac{2\operatorname{sech}^2(x)}{U_0}, \quad B^1 = \frac{4\operatorname{sech}^2(x)\tanh(x)}{V_0}.$$

Similarly, we can obtain additional coefficients by replacing various values of  $n$  in Equation (21). From Equations (19) and (20), we obtain the approximate solutions as follows:

$$U(x, t) = U_0(A^0 + \frac{A^1 t^\alpha}{\Gamma(\alpha + 1)} + \frac{A^2 t^{2\alpha}}{\Gamma(2\alpha + 1)} + \frac{A^3 t^{3\alpha}}{\Gamma(3\alpha + 1)} + \dots),$$

$$V(x, t) = V_0(B^0 + \frac{B^1 t^\alpha}{\Gamma(\alpha + 1)} + \frac{B^2 t^{2\alpha}}{\Gamma(2\alpha + 1)} + \frac{B^3 t^{3\alpha}}{\Gamma(3\alpha + 1)} + \dots).$$

- To implement the LADM, we take the Laplace transform of Equation (1); then,

$$\begin{cases} \mathcal{L}[\mathcal{D}_t^\alpha U] + \mathcal{L}[UU_x + V_x] = 0, \\ \mathcal{L}[\mathcal{D}_t^\alpha V] + \mathcal{L}[U_x + (UV)_x + U_{xxx}] = 0, \end{cases}$$

and by using the differential property of the Laplace transform, we have:

$$\begin{cases} \mathcal{L}[\mathcal{D}_t^\alpha U] = \frac{1}{s}U(x, 0) - \frac{1}{s^\alpha}\mathcal{L}[UU_x + V_x], \\ \mathcal{L}[\mathcal{D}_t^\alpha V] = \frac{1}{s}V(x, 0) - \frac{1}{s^\alpha}\mathcal{L}[U_x + (UV)_x + U_{xxx}]. \end{cases} \quad (22)$$

As in the LADM, the solution can be represented as an infinite series

$$\mathbf{U}(x, t) = \sum_{r=0}^{\infty} \mathbf{U}_r(x, t); \quad \mathbf{U} = (U, V)^T, \quad (23)$$

and the nonlinear term in Equation (1) can be decomposed as

$$N_1\mathbf{U}(x, t) = \sum_{r=0}^{\infty} \mathcal{A}_r, \quad N_2\mathbf{U}(x, t) = \sum_{r=0}^{\infty} \mathcal{B}_r,$$

where  $\mathcal{A}_r$  and  $\mathcal{B}_r$  are Adomian polynomials, which can be calculated by the following formulas:

$$\begin{cases} \mathcal{A}_r = \frac{1}{r!} \frac{d^r}{d\lambda^r} N_1 \left( \sum_{i=0}^{\infty} \lambda^i \mathbf{U}_i \right) \Big|_{\lambda=0}, \\ \mathcal{B}_r = \frac{1}{r!} \frac{d^r}{d\lambda^r} N_2 \left( \sum_{i=0}^{\infty} \lambda^i \mathbf{U}_i \right) \Big|_{\lambda=0}. \end{cases} \quad (24)$$

Substitution Equations (23) and (24) with ICs (2) into Equation (22) yields:

$$\begin{cases} \mathcal{L}[\sum_{r=0}^{\infty} U_r(x, t)] = \frac{1}{s}(1 + 2\tanh(x)) - \frac{1}{s^\alpha}\mathcal{L}[N_1 + \partial_x(\sum_{r=0}^{\infty} V_r(x, t))], \\ \mathcal{L}[\sum_{r=0}^{\infty} V_r(x, t)] = \frac{1}{s}(1 - 2\tanh^2(x)) - \frac{1}{s^\alpha}\mathcal{L}[\partial_x(\sum_{r=0}^{\infty} U_r(x, t)) + N_2 \\ + \partial_{xxx}(\sum_{r=0}^{\infty} U_r(x, t))]. \end{cases} \quad (25)$$

By applying the inverse Laplace transform on both sides of Equation (25), we obtain

$$\begin{cases} U_{r+1} = -\mathcal{L}^{-1}[\frac{1}{s^\alpha}\mathcal{L}[\mathcal{A}_r + V_x]], \\ V_{r+1} = -\mathcal{L}^{-1}[\frac{1}{s^\alpha}\mathcal{L}[U_x + \mathcal{B}_r + U_{xxx}]], \end{cases} \quad (26)$$

where

$$\begin{cases} U_0 = 1 + 2\tanh(x), \\ V_0 = 1 - 2\tanh^2(x). \end{cases}$$

The nonlinear terms  $\mathcal{A}_r$  and  $\mathcal{B}_r$  can be written as:

$$\mathcal{A}_0 = U_0 U_{0x}, \quad \mathcal{A}_1 = U_{0x} U_1 + U_0 U_{1x}, \quad \mathcal{A}_2 = U_{0x} U_2 + U_{1x} U_1 + U_0 U_{2x}, \dots \quad (27)$$

$$\mathcal{B}_0 = (U_0 V_0)_x, \quad \mathcal{B}_1 = (U_0 V_1 + V_0 U_1)_x, \quad \mathcal{B}_2 = (U_0 V_2 + U_1 V_1 + V_0 U_2)_x, \dots \quad (28)$$

In order to obtain the other terms of the projected solutions, we substitute the values of Equations (27) and (28) into Equation (26), yielding:

$$\begin{cases} U_1 = -2 \frac{t^\alpha}{\Gamma(\alpha+1)} \operatorname{sech}^2(x), & U_2 = -4 \frac{t^{2\alpha}}{\Gamma(2\alpha+1)} \operatorname{sech}^2(x) \tanh(x), \dots \\ V_1 = 4 \frac{t^\alpha}{\Gamma(\alpha+1)} \operatorname{sech}^2(x) \tanh(x), & V_2 = 4 \frac{t^{2\alpha}}{\Gamma(2\alpha+1)} [\cosh(2x) - 2] \operatorname{sech}^4(x), \dots \end{cases}$$

Finally, we approximate the analytic solution  $U(x, t)$  and  $V(x, t)$  by

$$U(x, t) = \lim_{r \rightarrow \infty} U_r(x, t) = U_0 + U_1 + U_3 + \dots,$$

$$V(x, t) = \lim_{r \rightarrow \infty} V_r(x, t) = V_0 + V_1 + V_3 + \dots$$

In Tables 1 and 2, the MGMLFM approximate solutions of Example 1 are shown for various values of  $\alpha$  and compared with the exact solution. The tabled results below seem to coincide with the values of the exact solution (18), which means that the MGMLFM is a more accurate technique than those methods that give a solution as an infinite series.

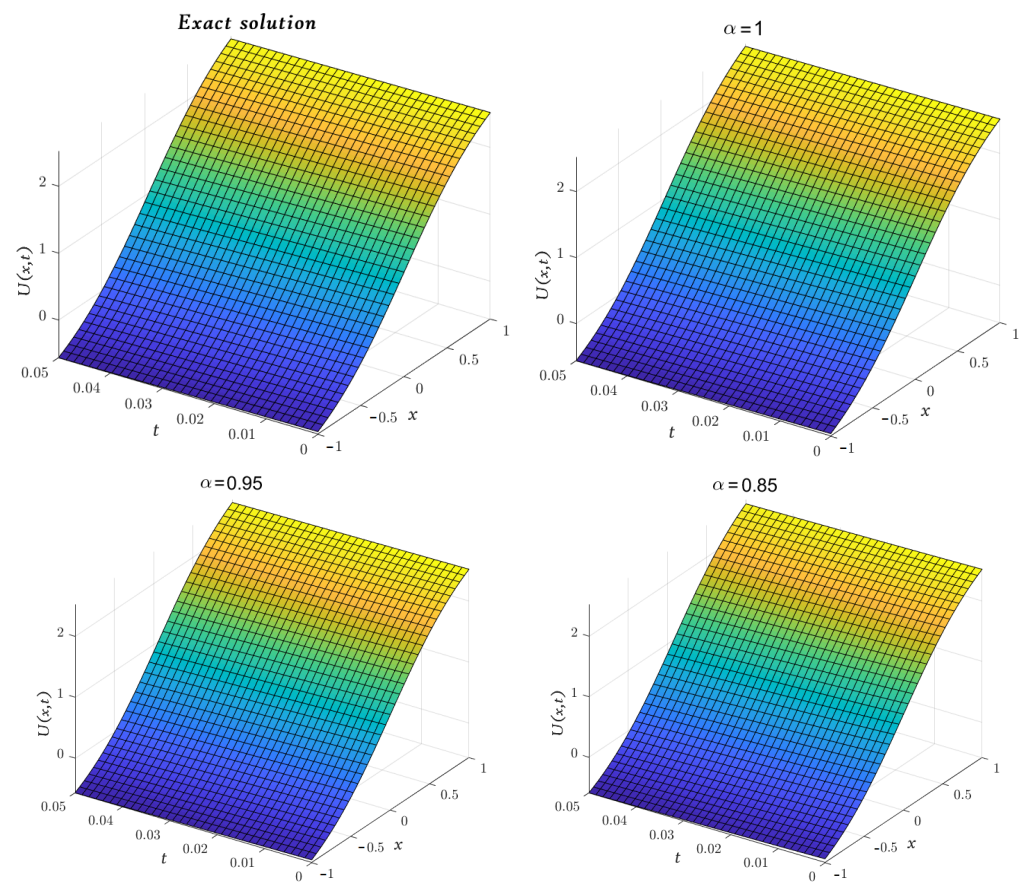
**Table 1.** Values of approximate solutions obtained by the MGMLFM, exact solution, and absolute errors of  $U(x, t)$  for system (1) with various values of  $\alpha, t$  and  $x$ .

$x$	$t$	$\alpha = 0.8$	$\alpha = 0.9$	$\alpha = 1$	Exact [48]	Absolute Error
		MGMLFM	MGMLFM	MGMLFM		
−1	0.003	−0.532386	−0.528021	−0.525748	−0.525702	$4.51907 \times 10^{-5}$
	0.006	−0.539882	−0.547092	−0.528385	−0.528205	$1.79812 \times 10^{-4}$
	0.009	−0.547092	−0.536834	−0.531099	−0.530696	$4.02448 \times 10^{-4}$
−0.5	0.003	0.0600753	0.0671357	0.0710849	0.0710535	$3.13711 \times 10^{-5}$
	0.006	0.0489784	0.0598679	0.0664763	0.0663545	$1.21755 \times 10^{-4}$
	0.009	0.0392715	0.0531238	0.0619344	0.0616686	$2.65732 \times 10^{-4}$
0.5	0.003	1.90859	1.91561	1.91955	1.91951	$4.53038 \times 10^{-5}$
	0.006	1.8977	1.90838	1.91495	1.91477	$1.80805 \times 10^{-4}$
	0.009	1.88838	1.90171	1.91043	1.91002	$4.05897 \times 10^{-4}$
1	0.003	2.51404	2.51836	2.52063	2.52066	$3.28798 \times 10^{-5}$
	0.006	2.50673	2.51397	2.518	2.51813	$1.2751 \times 10^{-4}$
	0.009	2.49988	2.50966	2.5153	2.51558	$2.78165 \times 10^{-4}$

In Figures 1 and 2 the LADM approximate solutions of  $U(x, t)$  and  $V(x, t)$  at various values of  $\alpha$  are plotted in the domain  $-1 < x < 1$ ,  $0 < t < 0.05$ ; Moreover, a 3D graph with comparative results at  $\alpha = 1, 0.8, 0.6, 0.4$  is shown.

**Table 2.** Values of approximate solutions obtained by the MGMLFM, exact solution, and absolute errors of  $V(x, t)$  for system (1) with various values of  $\alpha, t$  and  $x$ .

$x$	$t$	$\alpha = 0.8$	$\alpha = 0.9$	$\alpha = 1$	Exact [48]	Absolute Error
		MGMLFM	MGMLFM	MGMLFM		
-1	0.003	-0.172947	-0.167111	-0.16387	-0.163884	$1.3969 \times 10^{-5}$
	0.006	-0.182166	-0.173109	-0.16765	-0.167705	$5.5459 \times 10^{-5}$
	0.009	-0.190232	-0.178702	-0.171392	-0.171515	$1.23872 \times 10^{-4}$
-0.5	0.003	0.559953	0.56534	0.56868	0.568529	$1.50951 \times 10^{-4}$
	0.006	0.552808	0.559654	0.564751	0.564153	$5.98079 \times 10^{-4}$
	0.009	0.548031	0.554961	0.5611	0.559767	$1.33332 \times 10^{-3}$
0.5	0.003	0.588096	0.581064	0.577273	0.577252	$2.14755 \times 10^{-5}$
	0.006	0.599675	0.588242	0.581683	0.581597	$8.62386 \times 10^{-5}$
	0.009	0.610335	0.595142	0.586127	0.585932	$1.94798 \times 10^{-4}$
1	0.003	-0.148477	-0.153365	-0.156333	-0.156208	$1.25863 \times 10^{-4}$
	0.006	-0.141644	-0.148238	-0.152846	-0.152353	$4.93352 \times 10^{-4}$
	0.009	-0.136498	-0.143877	-0.149575	-0.148487	$1.08802 \times 10^{-3}$

**Figure 1.** Cont.

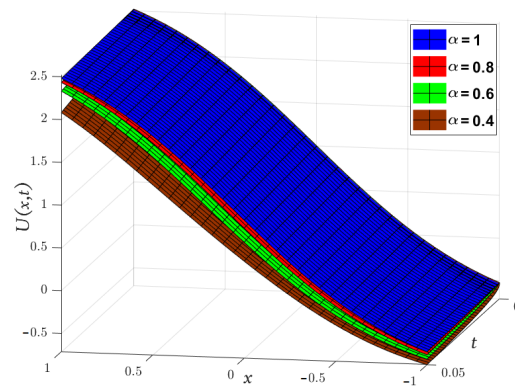


**Figure 1.** Three-dimensional plots of the approximate and exact solutions of  $U(x, t)$  (Example 1) using the LADM.

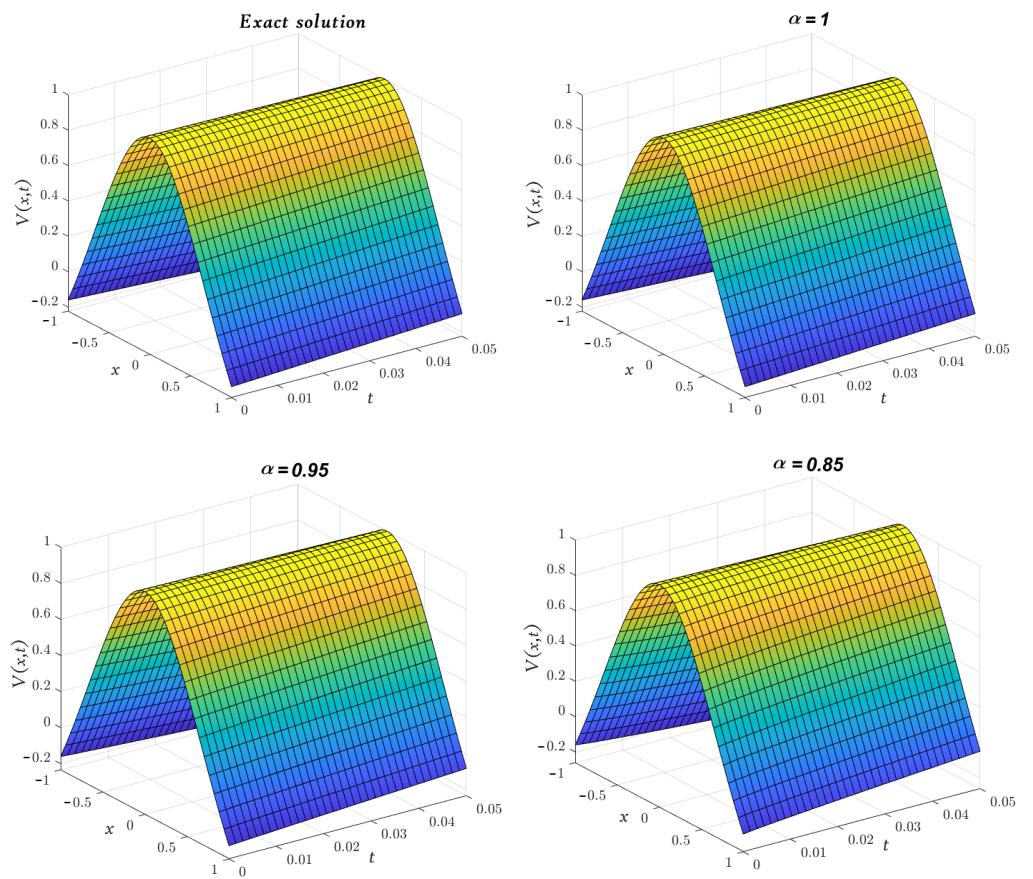


**Figure 2.** Cont.

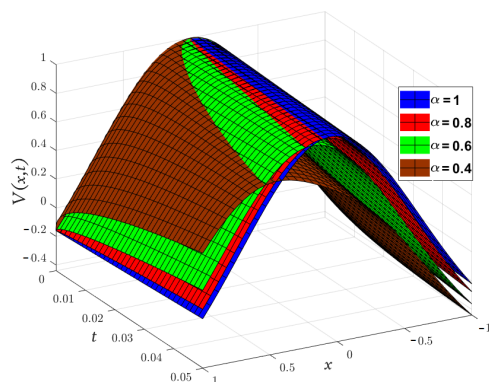


**Figure 2.** Three-dimensional plots of the approximate and exact solutions of  $V(x, t)$  (Example 1) using the LADM.

Figure 3 represents the 2D graphs of the exact solution and the LADM solutions of  $U(x, t)$  and  $V(x, t)$  for  $\alpha = 1, 0.95, 0.85$ , and  $x = 0.5$ .

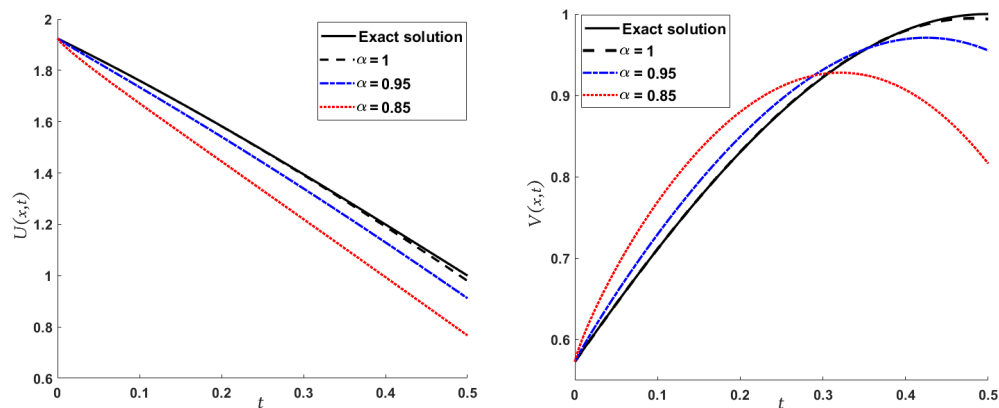


**Figure 3.** Two-dimensional plots of the approximate and exact solutions of  $U(x, t)$ ,  $V(x, t)$  (Example 1) using the LADM, when  $x = 0.5$ .

**Example 2.** Consider the system of NFPDEs (3) subject to ICs (4) and the known exact solutions of this system when  $\alpha = 1$  are given as [49]:

$$U(x, t) = \sin(x)e^{-t}, \quad V(x, t) = \sin(x)e^{-t}. \tag{29}$$

- We apply the MGMLFM, using the suggestions stated in (9); let

$$U(x, t) = \sum_{n=0}^{\infty} F_1(x)A^n \frac{t^{n\alpha}}{\Gamma(n\alpha + 1)}, \tag{30}$$

$$V(x, t) = \sum_{n=0}^{\infty} F_2(x)B^n \frac{t^{n\alpha}}{\Gamma(n\alpha + 1)}, \tag{31}$$

From ICs (4), we have  $F_1(x) = \sin(x)$  and  $F_2(x) = \sin(x)$ . By using Equation (11), we obtain the linear term of Equation (3) as follows:

$$\text{for } U(x, t) \rightarrow L(\sin(x)) = \frac{\partial^2 \sin(x)}{\partial x^2} = -\sin(x) \Rightarrow \lambda_1^* = -1,$$

$$\text{for } V(x, t) \rightarrow L(\sin(x)) = \frac{\partial^2 \sin(x)}{\partial x^2} = -\sin(x) \Rightarrow \lambda_2^* = -1.$$

Similarly, the nonlinear term of Equation (3) can be written as:

$$\begin{aligned} \text{for } U(x, t) \rightarrow N(\sin(x)) &= 2\sin(x) \frac{\partial \sin(x)}{\partial x} - \sin(x) \frac{\partial \sin(x)}{\partial x} - \sin(x) \frac{\partial \sin(x)}{\partial x} = 0, \\ \text{for } V(x, t) \rightarrow N(\sin(x)) &= 2\sin(x) \frac{\partial \sin(x)}{\partial x} - \sin(x) \frac{\partial \sin(x)}{\partial x} - \sin(x) \frac{\partial \sin(x)}{\partial x} = 0. \end{aligned}$$

By using Equations (3) and (10), we get:

$$\begin{aligned} \sin(x) \sum_{n=0}^{\infty} (A^{n+1} + A^n) \frac{t^{n\alpha}}{\Gamma(n\alpha + 1)} &= 0, \\ \sin(x) \sum_{n=0}^{\infty} (B^{n+1} + B^n) \frac{t^{n\alpha}}{\Gamma(n\alpha + 1)} &= 0. \end{aligned}$$

Then, the RR are given by:

$$A^{n+1} = -A^n, \quad B^{n+1} = -B^n.$$

By substituting values of  $n$ , we have:

$$\begin{aligned} A^0 &= 1, & B^0 &= 1, \\ A^1 &= -1, & B^1 &= -1, \\ A^2 &= 1, & B^2 &= 1 \\ A^3 &= -1, & B^3 &= -1. \end{aligned}$$

From Equations (30) and (31), we get:

$$\begin{aligned} U(x, t) &= \sin(x) \left( 1 - \frac{t^\alpha}{\Gamma(\alpha + 1)} + \frac{t^{2\alpha}}{\Gamma(2\alpha + 1)} - \frac{t^{3\alpha}}{\Gamma(3\alpha + 1)} + \dots \right) = \sin(x) E_\alpha(-t^\alpha), \\ V(x, t) &= \sin(x) \left( 1 - \frac{t^\alpha}{\Gamma(\alpha + 1)} + \frac{t^{2\alpha}}{\Gamma(2\alpha + 1)} - \frac{t^{3\alpha}}{\Gamma(3\alpha + 1)} + \dots \right) = \sin(x) E_\alpha(-t^\alpha). \end{aligned}$$

- To implement the LADM, we take the Laplace transform of both sides of Equation (3); then,

$$\begin{cases} \mathcal{L}[\mathcal{D}_t^\alpha U(x, t)] = \mathcal{L}[U_{xx} + 2UU_x - (UV)_x], \\ \mathcal{L}[\mathcal{D}_t^\alpha V(x, t)] = \mathcal{L}[V_{xx} + 2VV_x - (UV)_x], \end{cases}$$

using the properties of the Laplace transform, we obtain:

$$\begin{cases} \mathcal{L}[U(x, t)] = \frac{1}{s} U(x, 0) + \frac{1}{s^\alpha} \mathcal{L}[U_{xx} + 2UU_x - (UV)_x], \\ \mathcal{L}[V(x, t)] = \frac{1}{s} V(x, 0) + \frac{1}{s^\alpha} \mathcal{L}[V_{xx} + 2VV_x - (UV)_x]. \end{cases}$$

The next step in the LADM is to represent the solution as Equation (23), and the nonlinear terms  $UU_x$ ,  $VV_x$  and  $(UV)_x$  are decomposed as

$$N_1 \mathbf{U}(x, t) = \sum_{r=0}^{\infty} \mathcal{A}_r, \quad N_2 \mathbf{U}(x, t) = \sum_{r=0}^{\infty} \mathcal{B}_r, \quad N_3 \mathbf{U}(x, t) = \sum_{n=0}^{\infty} \mathcal{C}_n,$$

where  $\mathcal{A}_r$ ,  $\mathcal{B}_r$  and  $\mathcal{C}_r$  are Adomian polynomials and their components are defined as:

$$\begin{cases} \mathcal{A}_r = \frac{1}{r!} \frac{d^r}{d\lambda^r} N_1 \left( \sum_{i=0}^{\infty} \lambda^i \mathbf{U}_i \right) \Big|_{\lambda=0}, \\ \mathcal{B}_r = \frac{1}{r!} \frac{d^r}{d\lambda^r} N_2 \left( \sum_{i=0}^{\infty} \lambda^i \mathbf{U}_i \right) \Big|_{\lambda=0}, \\ \mathcal{C}_r = \frac{1}{r!} \frac{d^r}{d\lambda^r} N_3 \left( \sum_{i=0}^{\infty} \lambda^i \mathbf{U}_i \right) \Big|_{\lambda=0}. \end{cases} \tag{32}$$

From Equations (23) and (32) with ICs (4), we have:

$$\begin{cases} \mathcal{L}[\sum_{r=0}^{\infty} U_r(x, t)] = \frac{1}{s} \sin(x) + \frac{1}{s^\alpha} \mathcal{L}[\partial_{xx} (\sum_{r=0}^{\infty} U_r(x, t))] + 2N_1 - N_3, \\ \mathcal{L}[\sum_{r=0}^{\infty} V_r(x, t)] = \frac{1}{s} \sin(x) + \frac{1}{s^\alpha} \mathcal{L}[\partial_{xx} (\sum_{r=0}^{\infty} V_r(x, t))] + 2N_2 - N_3. \end{cases} \tag{33}$$

Applying the inverse Laplace transform on both sides of Equation (33), we get

$$\begin{cases} U_{r+1} = \mathcal{L}^{-1}[\frac{1}{s^\alpha} \mathcal{L}[U_{rxx} + 2\mathcal{A}_r - \mathcal{C}_r]], \\ V_{r+1} = \mathcal{L}^{-1}[\frac{1}{s^\alpha} \mathcal{L}[V_{rxx} + 2\mathcal{B}_r - \mathcal{C}_r]], \end{cases}$$

where

$$\begin{cases} U_0 = \sin(x), \\ V_0 = \sin(x). \end{cases}$$

For the other terms, we can write:

$$\begin{cases} U_1 = -\frac{t^\alpha}{\Gamma(\alpha + 1)} \sin(x), \quad U_2 = \frac{t^{2\alpha}}{\Gamma(2\alpha + 1)} \sin(x), \dots \\ V_1 = \frac{t^\alpha}{\Gamma(\alpha + 1)} \sin(x), \quad V_2 = \frac{t^{2\alpha}}{\Gamma(2\alpha + 1)} \sin(x), \dots \end{cases} \tag{34}$$

Finally, we approximate the analytic solution  $U(x, t)$  and  $V(x, t)$  by

$$\begin{aligned} U(x, t) &= \lim_{r \rightarrow \infty} U_r(x, t) = U_0 + U_1 + U_3 + \dots, \\ V(x, t) &= \lim_{r \rightarrow \infty} V_r(x, t) = V_0 + V_1 + V_3 + \dots \end{aligned}$$

Obviously, the results in Table 3 are very close to the exact solution shown earlier in Equation (29) when  $\alpha = 1$ , which means that the approximate solutions obtained by the MGMLFM are rapidly converging to the exact solutions. Now, the LADM solutions for system (3) with ICs (4) are illustrated by the following simulation.

**Table 3.** Values of approximate solutions obtained by MGMLFM, FNDM, exact solution, and absolute errors of  $U(x, t)$  and  $V(x, t)$  for system (3) with various values of  $\alpha, t, x$  and  $\gamma = 0.4$ .

$x$	$t$	$\alpha = 0.75$		$\alpha = 0.9$		$\alpha = 1$		Exact	Absolute Error
		FNDM [49]	MGMLFM	FNDM [49]	MGMLFM	FNDM [49]	MGMLFM		
-10	0.2	0.403596	0.3985421	0.429046	0.4274714	0.446097	0.4454068	0.445407	$1.3478525 \times 10^{-9}$
	0.4	0.349827	0.3275878	0.358413	0.3487726	0.369934	0.3646684	0.364668	$1.6838537 \times 10^{-7}$
-5	0.2	0.711403	0.7024943	0.756262	0.7534867	0.786318	0.7851008	0.785101	$2.3758057 \times 10^{-9}$
	0.4	0.616625	0.5774259	0.63176	0.6147676	0.652069	0.6427865	0.642786	$2.9680616 \times 10^{-7}$
5	0.2	-0.711403	-0.7024943	-0.756262	-0.7534867	-0.786318	-0.7851008	-0.785101	$2.3758057 \times 10^{-9}$
	0.4	-0.616625	-0.5774259	-0.63176	-0.6147676	-0.652069	-0.6427865	-0.642786	$2.9680616 \times 10^{-7}$
10	0.2	-0.403596	-0.3985421	-0.429046	-0.4274714	-0.446097	-0.4454068	-0.445407	$1.3478525 \times 10^{-9}$
	0.4	-0.349827	-0.3275878	-0.358413	-0.3487726	-0.369934	-0.3646684	-0.364668	$1.6838537 \times 10^{-7}$

In Figure 4, we compare the obtained solutions by the LADM for  $U(x, t)$  and  $V(x, t)$  with the exact solution (29). Moreover, this figure illustrates the results obtained by the LADM for  $U(x, t)$  and  $V(x, t)$  with  $\alpha = 1, 0.8, 0.6, 0.4$ .

Further, in Figure 5, we display the comparison between exact and approximate solutions in two dimensions with time  $0 < t < 2, x = 1$ , (right figure) and with various values of space  $-10 < x < 10, t = 1$ , (left figure). Finally, it is noticeable that the LADM and MGMLFM approximate solutions overlap (for any interval of the variables  $x, t$ ) and have a high degree of accuracy when compared to the exact solution.

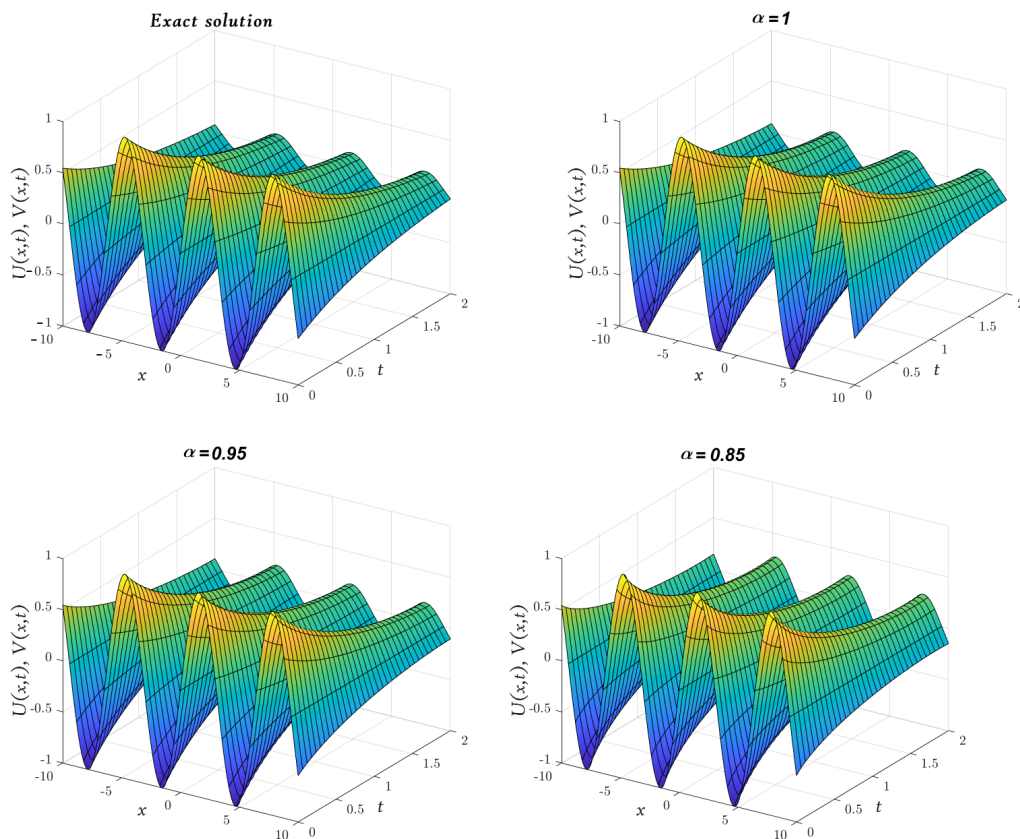
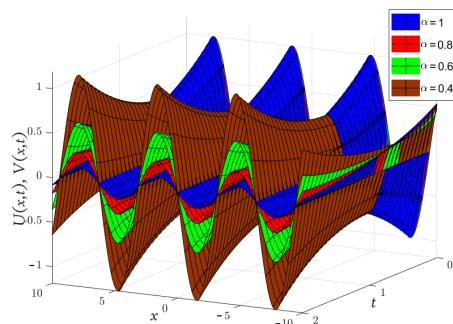


Figure 4. Cont.



**Figure 4.** Three-dimensional plots of the approximate and exact solutions of  $U(x,t)$ ,  $V(x,t)$  (Example 2) using the LADM.

**Example 3.** Consider the system (5) subject to ICs (6) and the known exact solutions of this system when  $\alpha = 1$  are given as [49,58]:

$$U(x,y,t) = e^{x+y-t}, \quad V(x,y,t) = e^{x-y+t}, \quad W(x,y,t) = e^{-x+y+t}. \quad (35)$$

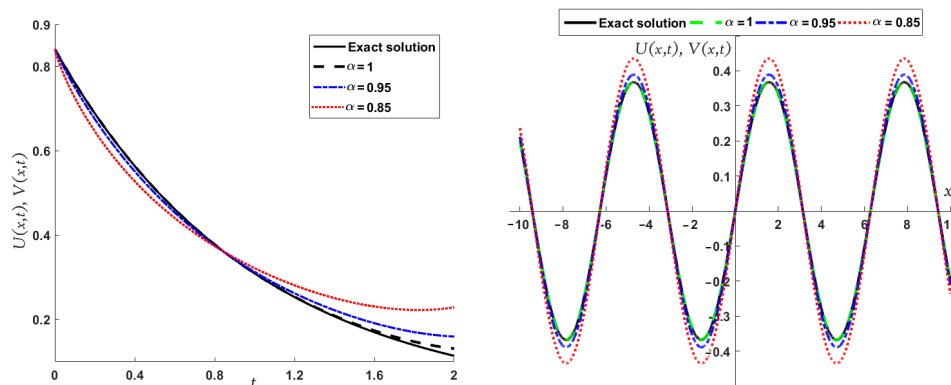


**Figure 5.** Two-dimensional plots of the approximate and exact solutions of  $U(x,t)$ ,  $V(x,t)$  (Example 2) using the LADM, when  $x = 1$  (right figure) and  $t = 1$  (left figure).

- To apply the MGMLFM, we assume

$$\begin{aligned}
 U(x,y,t) &= \sum_{n=0}^{\infty} F_1(x,y) A^n \frac{t^{n\alpha}}{\Gamma(n\alpha + 1)}, \\
 V(x,y,t) &= \sum_{n=0}^{\infty} F_2(x,y) B^n \frac{t^{n\alpha}}{\Gamma(n\alpha + 1)}, \\
 W(x,y,t) &= \sum_{n=0}^{\infty} F_3(x,y) S^n \frac{t^{n\alpha}}{\Gamma(n\alpha + 1)},
 \end{aligned}$$

where  $A$ ,  $B$ , and  $S$  are undetermined coefficients. From ICs (6), we have  $F_1(x,y) = e^{x+y}$ ,  $F_2(x,y) = e^{x-y}$ , and  $F_3(x,y) = e^{-x+y}$ . Similarly, as in Example 2, we calculate the linear and nonlinear parts of the system (5) and using Equation (10), we get

$$\begin{aligned}
 \sum_{n=0}^{\infty} (A^{n+1} - \lambda_1^* A^n) \frac{t^{n\alpha}}{\Gamma(n\alpha + 1)} &= 0, \\
 \sum_{n=0}^{\infty} (B^{n+1} - \lambda_2^* B^n) \frac{t^{n\alpha}}{\Gamma(n\alpha + 1)} &= 0, \\
 \sum_{n=0}^{\infty} (S^{n+1} - \lambda_3^* S^n) \frac{t^{n\alpha}}{\Gamma(n\alpha + 1)} &= 0,
 \end{aligned} \quad (36)$$

where  $\lambda_1^* = -1, \lambda_2^* = 1, \text{ and } \lambda_3^* = 1$ . Then, the RR are given by

$$\begin{aligned} A^{n+1} &= \lambda_1^* A^n, \\ B^{n+1} &= \lambda_2^* B^n, \\ S^{n+1} &= \lambda_3^* S^n. \end{aligned}$$

By substituting different values of  $n$  and using Equation (36) we get the approximate solutions in the following:

$$\begin{aligned} U(x, y, t) &= e^{x+y} \left( 1 - \frac{t^\alpha}{\Gamma(\alpha + 1)} + \frac{t^{2\alpha}}{\Gamma(2\alpha + 1)} - \frac{t^{3\alpha}}{\Gamma(3\alpha + 1)} + \dots \right) = e^{x+y} E_\alpha(-t^\alpha), \\ V(x, y, t) &= e^{x-y} \left( 1 + \frac{t^\alpha}{\Gamma(\alpha + 1)} + \frac{t^{2\alpha}}{\Gamma(2\alpha + 1)} + \frac{t^{3\alpha}}{\Gamma(3\alpha + 1)} + \dots \right) = e^{x-y} E_\alpha(t^\alpha), \\ W(x, y, t) &= e^{-x+y} \left( 1 + \frac{t^\alpha}{\Gamma(\alpha + 1)} + \frac{t^{2\alpha}}{\Gamma(2\alpha + 1)} + \frac{t^{3\alpha}}{\Gamma(3\alpha + 1)} + \dots \right) = e^{-x+y} E_\alpha(t^\alpha). \end{aligned}$$

- To implement the LADM, we take the Laplace transform of Equation (5),

$$\begin{cases} \mathcal{L}[\mathcal{C}\mathcal{D}_t^\alpha U(x, y, t)] = \mathcal{L}[W_x V_y - W_y V_x - U], \\ \mathcal{L}[\mathcal{C}\mathcal{D}_t^\alpha V(x, y, t)] = \mathcal{L}[V - U_y W_x - U_x W_y], \\ \mathcal{L}[\mathcal{C}\mathcal{D}_t^\alpha W(x, y, t)] = \mathcal{L}[W - V_y U_x - V_x U_y], \end{cases}$$

using the Laplace transform of the Caputo derivative, we have

$$\begin{cases} \mathcal{L}[U(x, y, t)] = \frac{1}{s} U(x, y, 0) + \frac{1}{s^\alpha} \mathcal{L}[W_x V_y - W_y V_x - U], \\ \mathcal{L}[V(x, y, t)] = \frac{1}{s} V(x, y, 0) + \frac{1}{s^\alpha} \mathcal{L}[V - U_y W_x - U_x W_y], \\ \mathcal{L}[W(x, y, t)] = \frac{1}{s} W(x, y, 0) + \frac{1}{s^\alpha} \mathcal{L}[W - V_y U_x - V_x U_y]. \end{cases} \tag{37}$$

Representing the solution  $U(x, y, t), V(x, y, t), \text{ and } W(x, y, t)$  as an infinite series, as follows,

$$\mathbf{U}(x, y, t) = \sum_{r=0}^{\infty} \mathbf{U}_r(x, y, t); \quad \mathbf{U} = (U, V, W)^T, \tag{38}$$

the nonlinear terms included in Equation (5) can be decomposed as

$$\begin{aligned} N_1 \mathbf{U}(x, y, t) &= \sum_{r=0}^{\infty} \mathcal{A}_r, & N_2 \mathbf{U}(x, y, t) &= \sum_{r=0}^{\infty} \mathcal{A}_r^*, \\ N_3 \mathbf{U}(x, y, t) &= \sum_{n=0}^{\infty} \mathcal{B}_n, & N_4 \mathbf{U}(x, y, t) &= \sum_{r=0}^{\infty} \mathcal{B}_r^*, \\ N_4 \mathbf{U}(x, y, t) &= \sum_{n=0}^{\infty} \mathcal{C}_n, & N_5 \mathbf{U}(x, y, t) &= \sum_{r=0}^{\infty} \mathcal{C}_r^*, \end{aligned}$$

where  $\mathcal{A}_r, \mathcal{A}_r^*, \mathcal{B}_r, \mathcal{B}_r^*, \mathcal{C}_r$  and  $\mathcal{C}_r^*$  are Adomian polynomials defined as:

$$\begin{cases} \mathcal{A}_r = \frac{1}{r!} \frac{d^r}{d\lambda^r} N_1 \left( \sum_{i=0}^{\infty} \lambda^i \mathbf{U}_i \right) \Big|_{\lambda=0}, & \mathcal{A}_r^* = \frac{1}{r!} \frac{d^r}{d\lambda^r} N_2 \left( \sum_{i=0}^{\infty} \lambda^i \mathbf{U}_i \right) \Big|_{\lambda=0}, \\ \mathcal{B}_r = \frac{1}{r!} \frac{d^r}{d\lambda^r} N_3 \left( \sum_{i=0}^{\infty} \lambda^i \mathbf{U}_i \right) \Big|_{\lambda=0}, & \mathcal{B}_r^* = \frac{1}{r!} \frac{d^r}{d\lambda^r} N_4 \left( \sum_{i=0}^{\infty} \lambda^i \mathbf{U}_i \right) \Big|_{\lambda=0}, \\ \mathcal{C}_r = \frac{1}{r!} \frac{d^r}{d\lambda^r} N_5 \left( \sum_{i=0}^{\infty} \lambda^i \mathbf{U}_i \right) \Big|_{\lambda=0}, & \mathcal{C}_r^* = \frac{1}{r!} \frac{d^r}{d\lambda^r} N_6 \left( \sum_{i=0}^{\infty} \lambda^i \mathbf{U}_i \right) \Big|_{\lambda=0}. \end{cases} \quad (39)$$

From Equations (38) and (39) with ICs (6), Equation (37) becomes:

$$\begin{cases} \mathcal{L}[\sum_{r=0}^{\infty} U_r(x, y, t)] = \frac{1}{s} e^{x+y} + \frac{1}{s^\alpha} \mathcal{L}[N_1 - N_2 - \sum_{r=0}^{\infty} U_r(x, y, t)], \\ \mathcal{L}[\sum_{r=0}^{\infty} V_r(x, y, t)] = \frac{1}{s} e^{x-y} + \frac{1}{s^\alpha} \mathcal{L}[\sum_{r=0}^{\infty} V_r(x, y, t) - N_3 - N_4], \\ \mathcal{L}[\sum_{r=0}^{\infty} W_r(x, y, t)] = \frac{1}{s} e^{-x+y} + \frac{1}{s^\alpha} \mathcal{L}[\sum_{r=0}^{\infty} W_r(x, y, t) - N_5 - N_6]. \end{cases} \quad (40)$$

by apply the inverse Laplace transform to Equation (40), we get

$$\begin{cases} U_{r+1} = \mathcal{L}^{-1}[\frac{1}{s^\alpha} \mathcal{L}[\mathcal{A}_r - \mathcal{A}_r^* - U_r]], \\ V_{r+1} = \mathcal{L}^{-1}[\frac{1}{s^\alpha} \mathcal{L}[V_r - \mathcal{B}_r - \mathcal{B}_r^*]], \\ W_{r+1} = \mathcal{L}^{-1}[\frac{1}{s^\alpha} \mathcal{L}[W_r - \mathcal{C}_r - \mathcal{C}_r^*]], \end{cases}$$

where

$$\begin{cases} U_0 = e^{x+y}, \\ V_0 = e^{x-y}, \\ W_0 = e^{-x+y}. \end{cases}$$

Then, it follows that for the remaining terms we obtain the solution

$$\begin{cases} U_1 = \mathcal{L}^{-1}[\frac{1}{s^\alpha} \mathcal{L}[\mathcal{A}_0 - \mathcal{A}_0^* - U_0]] = -e^{x+y} \frac{t^\alpha}{\Gamma(\alpha + 1)}, \\ V_1 = \mathcal{L}^{-1}[\frac{1}{s^\alpha} \mathcal{L}[V_0 - \mathcal{B}_0 - \mathcal{B}_0^*]] = e^{x-y} \frac{t^\alpha}{\Gamma(\alpha + 1)}, \\ W_1 = \mathcal{L}^{-1}[\frac{1}{s^\alpha} \mathcal{L}[W_0 - \mathcal{C}_0 - \mathcal{C}_0^*]] = e^{-x+y} \frac{t^\alpha}{\Gamma(\alpha + 1)}. \end{cases}$$

The other terms of  $U_2, U_3, \dots, V_2, V_3, \dots$  and  $W_2, W_3, \dots$ , can be computed, respectively, in the same way and according to the ADM the solution is as follows:

$$\begin{aligned} U(x, y, t) &= \lim_{r \rightarrow \infty} U_r(x, y, t) = U_0 + U_1 + U_3 + \dots, \\ V(x, y, t) &= \lim_{r \rightarrow \infty} V_r(x, y, t) = V_0 + V_1 + V_3 + \dots, \\ W(x, y, t) &= \lim_{r \rightarrow \infty} W_r(x, y, t) = W_0 + W_1 + W_3 + \dots \end{aligned}$$

The results in Tables 4–6 coincide with the exact solutions described in Equation (35) when  $\alpha = 1$ . This confirms that the approximate solutions obtained by the MGMLFM are rapidly converging to the exact solutions and this is explained in the following tables.

**Table 4.** Values of approximate solutions obtained by MGMLFM, FNDM, exact solution, and absolute errors of  $U$  for system (5) with various values of  $\alpha, t, x$  and  $y = 0.4$ .

$x$	$t$	$\alpha = 0.75$		$\alpha = 0.9$		$\alpha = 1$		Exact	Absolute Error
		FNDM [49]	MGMLFM	FNDM [49]	MGMLFM	FNDM [49]	MGMLFM		
0.5	0.3	1.6256	1.6241897	1.74178	1.74158	1.82217	1.8221189	1.82212	$1.0285638 \times 10^{-7}$
	0.6	1.27791	1.2607914	1.31047	1.3063996	1.35131	1.3498715	1.34986	$1.27012 \times 10^{-5}$
	0.9	1.10414	1.033497	1.02931	1.0058445	1.0105	1.00021	1	$2.09565 \times 10^{-4}$
1	0.3	2.68017	2.6778362	2.8717	2.871385	3.00424	3.0041662	3.00417	$1.695815 \times 10^{-7}$
	0.6	2.10692	2.0786935	2.1606	2.1538889	2.22793	2.225562	2.22554	$2.09407 \times 10^{-5}$
	0.9	1.82042	1.7039486	1.69705	1.6583572	1.66603	1.649067	1.64872	$3.45514 \times 10^{-4}$
1.5	0.3	4.41885	4.4150055	4.73464	4.7341143	4.95316	4.9530327	4.95303	$2.7959262 \times 10^{-7}$
	0.6	3.47372	3.4271863	3.56223	3.5511624	3.6323	3.6693312	3.6693	$3.45253 \times 10^{-5}$
	0.9	3.00136	2.809336	2.79796	2.7341689	2.74682	2.718851	2.71828	$5.69657 \times 10^{-4}$

**Table 5.** Values of approximate solutions obtained by MGMLFM, FNDM, exact solution, and absolute errors of  $V$  for system (5) with various values of  $\alpha, t, x$  and  $y = 0.4$ .

$x$	$t$	$\alpha = 0.75$		$\alpha = 0.9$		$\alpha = 1$		Exact	Absolute Error
		FNDM [49]	MGMLFM	FNDM [49]	MGMLFM	FNDM [49]	MGMLFM		
0.5	0.3	1.76307	1.7638956	1.58084	1.5809426	1.4918	1.4918246	1.49182	$4.9816688 \times 10^{-8}$
	0.6	2.48848	2.5004130	2.17346	2.1758721	2.01296	2.0137461	2.01375	$6.6314571 \times 10^{-6}$
	0.9	3.40244	3.4604711	2.95156	2.9672968	2.71191	2.7181639	2.71828	$1.17976 \times 10^{-4}$
1	0.3	2.90682	2.9081722	2.60637	2.6065337	2.45956	2.4596030	2.4596	$8.2133832 \times 10^{-8}$
	0.6	4.10281	4.1224841	3.58343	3.5874066	3.31881	3.3201059	3.32012	$1.0933424 \times 10^{-5}$
	0.9	5.60968	5.7053523	4.86629	4.8922453	4.47118	4.4814946	4.48169	$1.9450873 \times 10^{-4}$
1.5	0.3	4.79253	4.7947653	4.29717	4.2974475	4.05514	4.0551998	4.0552	$1.3541579 \times 10^{-7}$
	0.6	6.76439	6.7968273	5.90808	5.9146336	5.47179	5.4739294	5.47395	$1.8026169 \times 10^{-5}$
	0.9	9.2488	9.4065356	8.02316	8.0659489	7.37174	7.3887354	7.38906	$3.2069069 \times 10^{-4}$

**Table 6.** Values of approximate solutions obtained by MGMLFM, FNDM, exact solution, and absolute errors of  $W$  for system (5) with various values of  $\alpha, t, x$  and  $y = 0.4$ .

$x$	$t$	$\alpha = 0.75$		$\alpha = 0.9$		$\alpha = 1$		Exact	Absolute Error
		FNDM [49]	MGMLFM	FNDM [49]	MGMLFM	FNDM [49]	MGMLFM		
0.5	0.3	1.44348	1.4441556	1.29428	1.2943663	1.22138	1.2214027	1.2214	$4.0786454 \times 10^{-8}$
	0.6	2.0374	2.0471650	1.77948	1.7814534	1.64807	1.6487158	1.64872	$5.4293779 \times 10^{-6}$
	0.9	2.78569	2.8331941	2.41653	2.4294171	2.22032	2.2254443	2.22554	$9.65902 \times 10^{-5}$
1	0.3	0.875516	0.8759246	0.785023	0.7850729	0.740807	0.7408182	0.740818	$2.4738235 \times 10^{-8}$
	0.6	1.23574	1.2416684	1.07931	1.0805061	0.999606	0.9999967	1	$3.2930841 \times 10^{-6}$
	0.9	1.6896	1.7184191	1.4657	1.4735159	1.34669	1.3498002	1.34986	$5.8584905 \times 10^{-5}$
1.5	0.3	0.531027	0.5312751	0.47614	0.4761708	0.449322	0.4493289	0.449329	$1.5004498 \times 10^{-8}$
	0.6	0.749516	0.7531099	0.654634	0.6553601	0.606291	0.6065287	0.606531	$1.9973565 \times 10^{-6}$
	0.9	1.0248	1.0422739	0.888992	0.8937326	0.816812	0.8186952	0.818731	$3.5533541 \times 10^{-5}$

In Figures 6–8, we compare the approximate solution obtained by the LADM for  $U(x, y, t)$ ,  $V(x, y, t)$ , and  $W(x, y, t)$  with the exact solution. Furthermore, Figure 9 represents the solutions obtained by the LADM for  $U(x, y, t)$ ,  $V(x, y, t)$ , and  $W(x, y, t)$  with various values of  $\alpha, y = 0.4$  and  $x = 1$ .

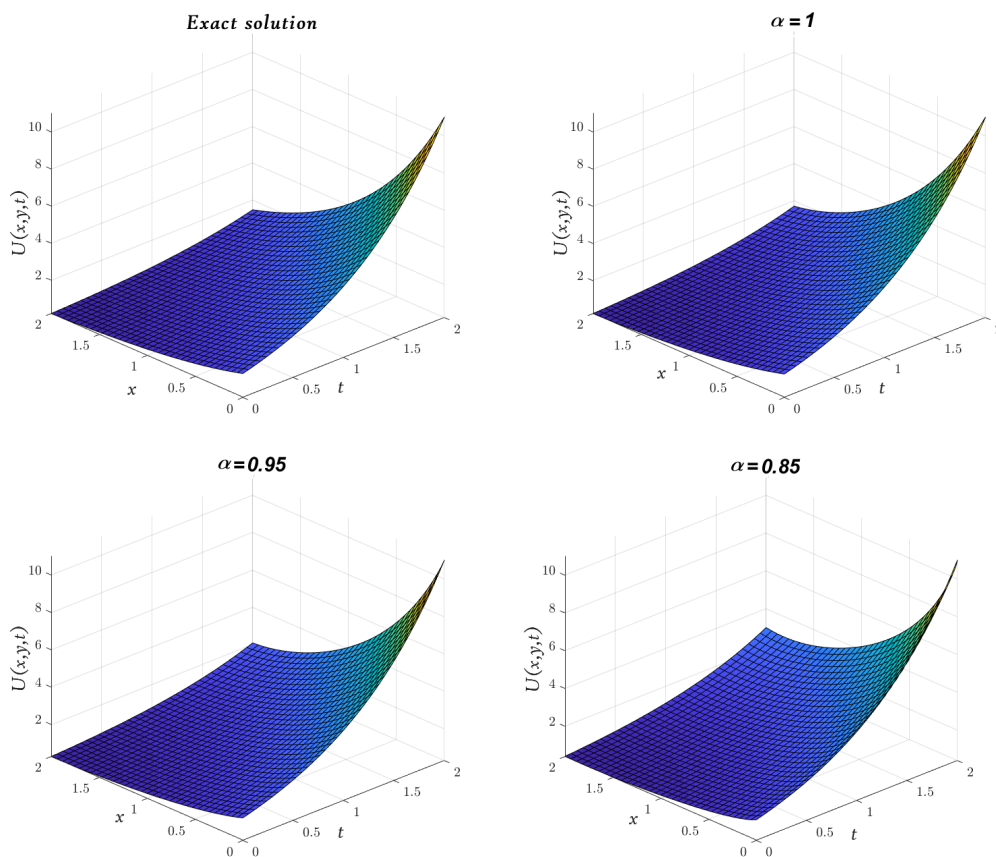


**Figure 6.** Cont.

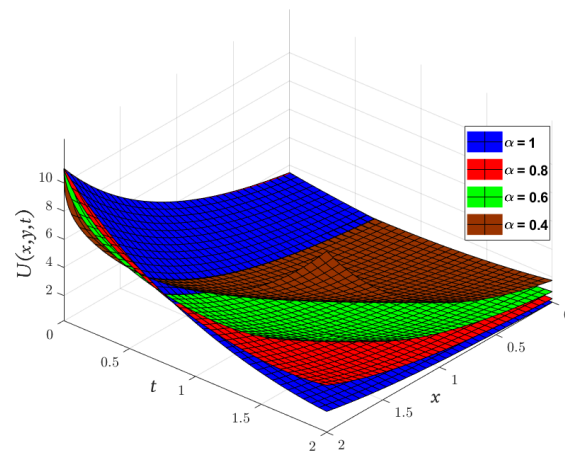


**Figure 6.** Three-dimensional plots of the approximate and exact solutions of  $U(x, y, t)$  (Example 3) using the LADM.

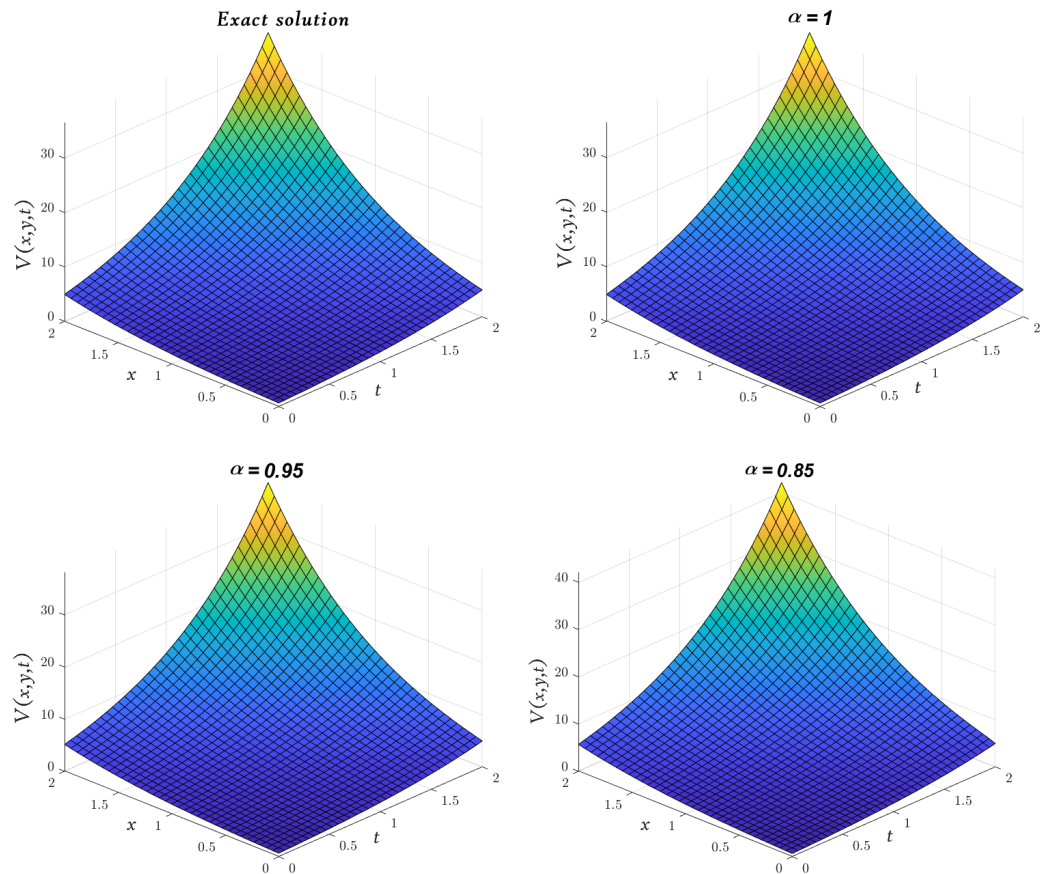


**Figure 7.** Cont.

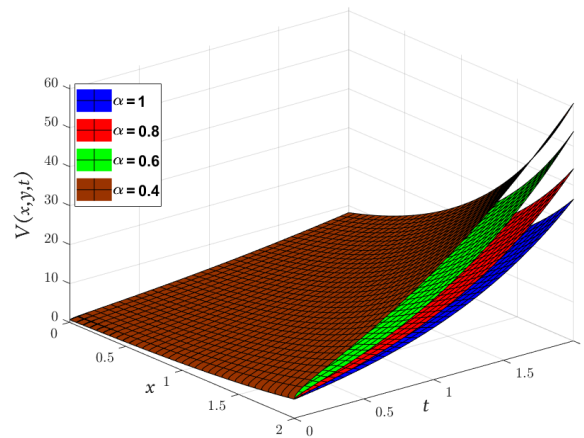


**Figure 7.** Three-dimensional plots of the approximate and exact solutions of  $V(x, y, t)$  (Example 3) using the LADM.

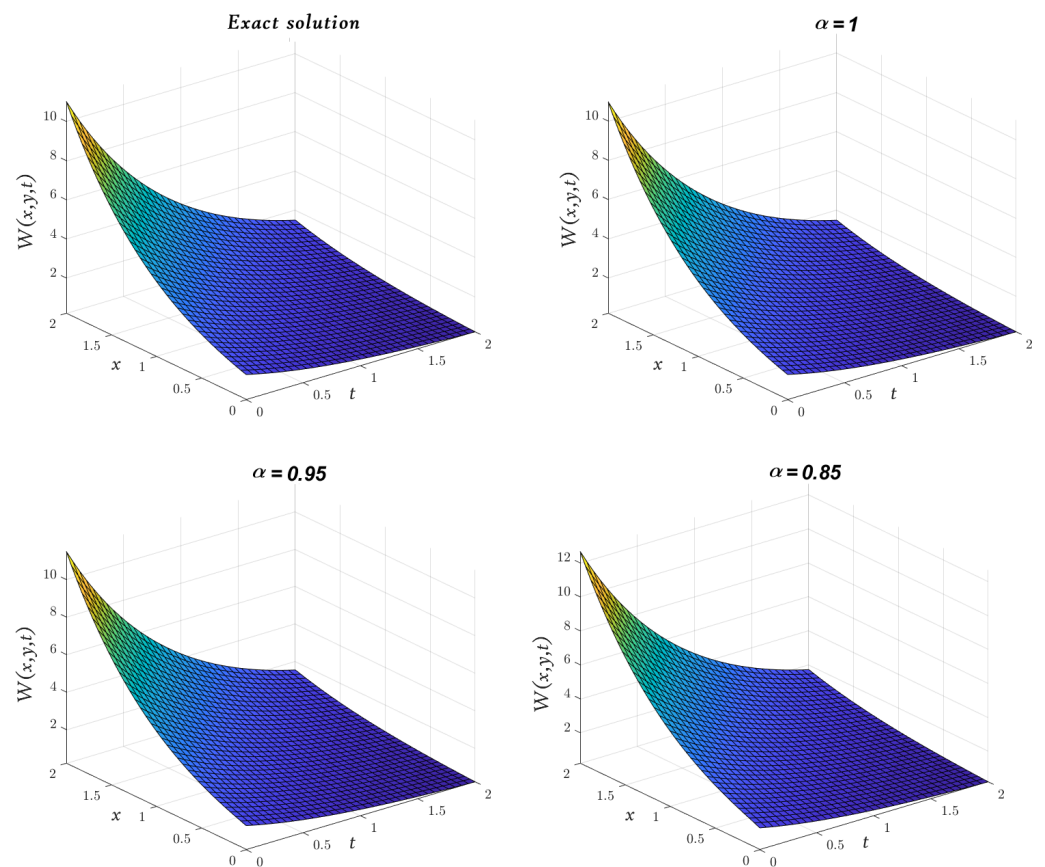


**Figure 8.** Cont.

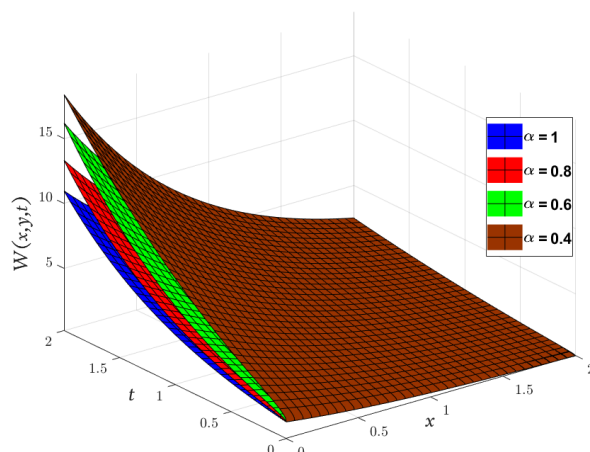


**Figure 8.** Three-dimensional plots of the approximate and exact solutions of  $W(x, y, t)$  (Example 3) using the LADM.

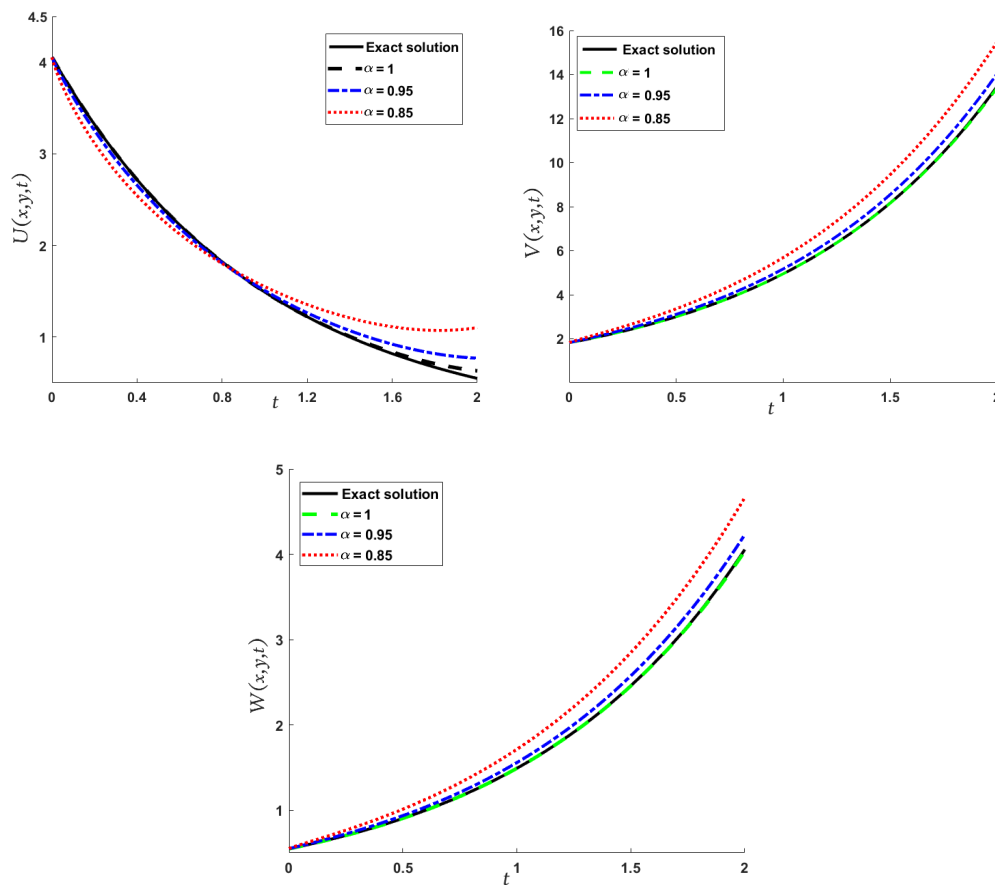


**Figure 9.** Two-dimensional plots of the approximate and exact solutions of  $U(x, y, t)$ ,  $V(x, y, t)$ ,  $W(x, y, t)$  (Example 3) using the LADM, when  $y = 0.4$  and  $x = 1$ .

**5. Conclusions**

In this article, the MGMLFM and LADM were successfully used to find analytic-approximate solutions for the NFPDEs. Moreover, we focused on solving fractional-order Broer–Kaup and Burgers’ systems that arise in many physical applications, and displayed our contributions in tables and figures for different domains of  $x, t$ . The LADM and MGMLFM solutions were presented at different values of  $\alpha$  and also for classical case (i.e.,  $\alpha = 1$ ), which showed a highly coincide with the exact solutions for all considered

problems. The analysis and computations confirmed that the approximate solutions offered by the MGMLFM and LADM had rapid convergence, required low computational cost, and provided highly accurate results compared to other analytical methods. Briefly, the obtained results together with their graphical simulations revealed the complete efficiency and accuracy of the proposed methods.

Our results motivate us to deal with other types of NFPDEs. For example, in the future, the used methods can be implemented to get the analytic-approximate solution for systems of NFPDEs that arise widely in the mathematical formulation of epidemiological models for different populations.

**Author Contributions:** Conceptualization, H.M.A. and I.G.A.; formal analysis, I.G.A., S.A. and H.M.A.; investigation, H.M.A. and I.G.A.; methodology, H.M.A. and I.G.A.; resources, I.G.A. and H.M.A.; software, I.G.A. and H.M.A.; validation, H.M.A. and I.G.A.; visualization, H.M.A. and I.G.A.; writing—original draft, I.G.A. and H.M.A.; writing—review and editing, H.M.A., H.A. and I.G.A.; writing-revised draft, S.A.; data curation, H.A.; project administration, H.A.; funding acquisition, S.A.; All authors have read and agreed to the published version of the manuscript.

**Funding:** This research received no external funding.

**Data Availability Statement:** Data can be provided on request.

**Acknowledgments:** Research Supporting Project number (RSP-2021/167), King Saud University, Riyadh, Saudi Arabia.

**Conflicts of Interest:** The authors declare no conflict of interest regarding the publication of this paper.

## References

1. Tarasov, V.E. Non-Linear Macroeconomic Models of Growth with Memory. *Mathematics* **2020**, *8*, 2078. [[CrossRef](#)]
2. Sardar, T.; Rana, S.; Bhattacharya, S.; Al-Khaled, K.; Chattopadhyay, J. A generic model for a single strain mosquito-transmitted disease with memory on the host and the vector. *Math. Biosci.* **2015**, *263*, 18–36. [[CrossRef](#)] [[PubMed](#)]
3. Tarasov, V.E. No nonlocality. No fractional derivative. *Commun. Nonlinear Sci. Numer. Simul.* **2018**, *62*, 157–163. [[CrossRef](#)]
4. Ameen, I. Fractional Calculus: Numerical Methods and SIR Models. Ph.D. Thesis, University of Padova, Padova, Italy, 2017.
5. Tuan, N.H.; Tri, V.V.; Baleanu, D. Analysis of the fractional corona virus pandemic via deterministic modeling. *Math. Meth. Appl. Sci.* **2021**, *44*, 1086–1102. [[CrossRef](#)]
6. Kumar, S.; Ahmadian, A.; Kumar, R.; Kumar, D.; Singh, J.; Baleanu, D.; Salimi, M. An Efficient Numerical Method for Fractional SIR Epidemic Model of Infectious Disease by Using Bernstein Wavelets. *Mathematics* **2020**, *8*, 558. [[CrossRef](#)]
7. Baleanu, D.; Agarwal, R.P. Fractional calculus in the sky. *Adv. Differ. Equ.* **2021**, *2021*, 117. [[CrossRef](#)]
8. Tarasov, V.E. Fractional vector calculus and fractional Maxwell's equations. *Ann. Phys.* **2008**, *323*, 2756–2778. [[CrossRef](#)]
9. West, B.J.; Turalskal, M.; Grigolini, P. Fractional calculus ties the microscopic and macroscopic scales of complex network dynamics. *New J. Phys.* **2015**, *17*, 045009. [[CrossRef](#)]
10. Scalar, E.; Gorenflo, R.; Mainardi, F. Fractional calculus and continuous time finance. *Physica A* **2000**, *284*, 376–384. [[CrossRef](#)]
11. Ameen, I.; Ali, H.M.; Alharthi, M.; Abdel-Aty, A.-H.; Elshehabey, H.M. Investigation of the dynamics of COVID-19 with a fractional mathematical model: A comparative study with actual data. *Res. Phys.* **2021**, *23*, 103976. [[CrossRef](#)]
12. Ameen, I.; Sweilam, N.; Ali, H.M. A fractional-order model of human liver: Analytic-approximate and numerical solutions comparing with clinical data. *Alex. Eng. J.* **2021**, *60*, 4797–4808. [[CrossRef](#)]
13. Ali, H.M.; Ameen, I. Optimal control strategies of a fractional order model for zika virus infection involving various transmissions. *Chaos Solitons Fractals* **2021**, *146*, 110864. [[CrossRef](#)]
14. Ameen, I.; Baleanu, D.; Ali, H.M. An efficient algorithm for solving the fractional optimal control of SIRV epidemic model with a combination of vaccination and treatment. *Chaos Solitons Fractals* **2020**, *137*, 109892. [[CrossRef](#)]
15. Hilfer, R. *Applications of Fractional Calculus in Physics*; World Scientific: Singapore, 2000.
16. Jaradat, A.; Noorani, M.S.M.; Alquran, M.; Jaradat, H.M. A novel method for solving Caputo-time-fractional dispersive long wave Wu-Zhang system. *Nonlinear Dyn. Syst. Theory* **2018**, *18*, 182–190.
17. Ali, H.M.; Pereira, F.L.; Gama, S. A new approach to the Pontryagin maximum principle for nonlinear fractional optimal control problems. *Math. Meth. Appl. Sci.* **2016**, *39*, 3640–3649. [[CrossRef](#)]
18. Syam, M.I.; Jaradat, H.M.; Alquran, M.; Al-Shara, S. An accurate method for solving a singular second-order fractional Emden-Fowler problem. *Adv. Differ. Equ.* **2018**, *2018*, 30. [[CrossRef](#)]
19. Alquran, M.; Jaradat, I. A novel scheme for solving Caputo time-fractional nonlinear equations: Theory and application. *Nonlinear Dyn.* **2018**, *91*, 2389–2395. [[CrossRef](#)]
20. Dhaigude, D.B.; Birajdar, G.A. Numerical Solution of Fractional Partial Differential Equations by Discrete Adomian Decomposition Method. *Adv. Appl. Math. Mech.* **2014**, *6*, 107–119. [[CrossRef](#)]

21. He, J.H. A short remark on fractional variational iteration method. *Phys. Lett. A* **2011**, *375*, 3362–3364. [[CrossRef](#)]
22. AL-Saif, A.S.J.; Hattim, T.A.K. Variational iteration method for solving some models of nonlinear partial differential equations. *Int. J. Pure Appl. Sci. Technol.* **2011**, *4*, 30–40.
23. Alao, S.; Oderinu, R.A.; Akinpelu, F.O.; Akinola, E.I. Homotopy analysis decomposition method for the solution of viscous boundary layer flow due to a moving sheet. *J. Adv. Math. Comput. Sci.* **2019**, *32*, 1–7. [[CrossRef](#)]
24. Arafa, A.A.M.; Rida, S.Z.; Mohamed, H. Approximate analytical solutions of Schnakenberg systems by homotopy analysis method. *Appl. Math. Mod.* **2012**, *36*, 4789–4796. [[CrossRef](#)]
25. Arafa, A.A.M.; Rida, S.Z.; Mohamed, H. An application of the homotopy analysis method to the transient behavior of a biochemical reaction model. *Inf. Sci. Lett.* **2014**, *3*, 29–33. [[CrossRef](#)]
26. Arafa, A.A.M.; Rida, S.Z.; Mohamed, H. Homotopy analysis method for solving biological population model. *Commun. Theor. Phys.* **2011**, *56*, 797–800. [[CrossRef](#)]
27. Javeed, S.; Baleanu, D.; Waheed, A.; Khan, M.S.; Affan, H. Analysis of homotopy perturbation method for solving fractional order differential equations. *Mathematics* **2019**, *7*, 40. [[CrossRef](#)]
28. He, J.H. Application of homotopy perturbation method to nonlinear wave equation. *Chaos Solitons Fractals* **2005**, *26*, 695–700. [[CrossRef](#)]
29. Ganji, D.D.; Sadighi, A. Application of homotopy perturbation and variational iteration methods to nonlinear heat transfer and porous media equations. *J. Comput. Appl. Math.* **2007**, *207*, 699–708. [[CrossRef](#)]
30. Arafa, A.A.M.; Rida, S.Z.; Mohammedin, A.A.; Ali, H.M. Solving nonlinear fractional differential equation by generalized Mittag–Leffler function method. *Commun. Theor. Phys.* **2013**, *59*, 661–663. [[CrossRef](#)]
31. Ali, H.M. New approximate solutions to fractional smoking model using the generalized Mittag–Leffler function method. *Progr. Fract. Differ. Appl.* **2019**, *5*, 319–326.
32. Mahdy, A.M.S.; Sweilam, N.H.; Higazy, M. Approximate solution for solving nonlinear fractional order smoking model. *Alex. Eng. J.* **2020**, *59*, 739–752. [[CrossRef](#)]
33. Arafa, A.A.M.; Rida, S.Z.; Ali, H.M. Generalized Mittag–Leffler function method for solving Lorenz system. *Inter. J. Innov. Appl. Stud.* **2013**, *3*, 105–111.
34. Suresh, P.L.; Piriadarshani, D. Mittag–Leffler function method for solving nonlinear Riccati differential equation with fractional order. *JCMCC* **2020**, *112*, 287–296.
35. Liu, Y.; Sun, H.; Yin, X.; Xin, B. A new Mittag–Leffler function undetermined coefficient method and its applications to fractional homogeneous partial differential equations. *J. Nonlinear Sci. Appl.* **2017**, *10*, 4515–4523. [[CrossRef](#)]
36. Ali, H.M. An efficient approximate-analytical method to solve time-fractional KdV and KdVB equations. *Inf. Sci. Lett.* **2020**, *9*, 189–198.
37. Ali, H.M.; Ameen, I. An efficient approach for solving fractional dynamics of a Predator-Prey system. *Mod. Appl. Sci.* **2019**, *13*, 116–126.
38. Adomian, G. A review of the decomposition method in applied mathematics. *Math. Anal. Appl.* **1988**, *135*, 501–544. [[CrossRef](#)]
39. Adomian, G.; Rach, R. Multiple decomposition for computational convenience. *Appl. Math. Lett.* **1990**, *3*, 97–99.
40. Adomian, G. Solving frontier problems of physics. In *The Decomposition Method, with a Preface by Yves Cherruault, Fundamental Theories of Physics*; Kluwer Academic Publishers Group: Dordrecht, The Netherlands, 1994.
41. Mohamed, M.Z.; Elzaki, T.M. Comparison between the Laplace Decomposition Method and Adomian Decomposition in Time-Space Fractional Nonlinear Fractional Differential Equations. *Appl. Math.* **2018**, *9*, 448–458. [[CrossRef](#)]
42. Xu, J.; Khan, H.; Shah, R.; Alderremy, A.A.; Aly, S.; Baleanu, D. The analytical analysis of nonlinear fractional-order dynamical models. *AIMS Math.* **2021**, *6*, 6201–6219. [[CrossRef](#)]
43. Haq, F.; Shah, K.; Al-Mdallal, Q.M.; Jarad, F. Application of a hybrid method for systems of fractional order partial differential equations arising in the model of the one-dimensional KellerSegel equation. *Eur. Phys. J. Plus* **2019**, *134*, 461. [[CrossRef](#)]
44. Mahmood, S.; Shah, R.; Arif, M. Laplace adomian decomposition method for multi dimensional time fractional model of Navier–Stokes equation. *Symmetry* **2019**, *11*, 149. [[CrossRef](#)]
45. Ali, A.; Humaira, L.; Shah, K. Analytical solution of general fishers equation by using Laplace Adomian decomposition method. *J. Pure Appl. Math.* **2018**, *2*, 1–4.
46. Khan, H.; Shah, R.; Kumam, P.; Baleanu, D.; Arif, M. An efficient analytical technique, for the solution of fractional-order telegraph equations. *Mathematics* **2019**, *7*, 426. [[CrossRef](#)]
47. Shah, R.; Khan, H.; Arif, M.; Kumam, P. Application of LaplaceAdomian decomposition method for the analytical solution of third-order dispersive fractional partial differential equations. *Entropy* **2019**, *21*, 335. [[CrossRef](#)] [[PubMed](#)]
48. Rawashdeh, M. Approximate solutions for coupled systems of nonlinear PDES using the reduced differential transform method. *Math. Comput. Appl.* **2019**, *19*, 161–171. [[CrossRef](#)]
49. Rawashdeh, M.S.; Al-Jammal, H. New approximate solutions to fractional nonlinear systems of partial differential equations using the FNDM. *Adv. Differ. Equ.* **2016**, *2016*, 235. [[CrossRef](#)]
50. Kilbas, A.A.A.; Srivastava, H.M.; Trujillo, J.J. *Theory and Applications of Fractional Differential Equations*; Elsevier Science Limited: New York, NY, USA, 2006; p. 204.
51. Podlubny, I. *Fractional Differential Equations, Mathematics in Sciences and Engineering*; Academic Press: San Diego, CA, USA, 1999.
52. Miller, K.S.; Ross, B. *An Introduction to the Fractional Calculus and Fractional Differential Equations*; Wiley: Hoboken, NJ, USA, 1993.

53. Khuri, S.A. A Laplace decomposition algorithm applied to a class of nonlinear differential equations. *J. Appl. Math.* **2001**, *1*, 141–155. [[CrossRef](#)]
54. Ghorbani, A. Beyond Adomian polynomials: He polynomials. *Chaos Solitons Fractals* **2009**, *39*, 1486–1492. [[CrossRef](#)]
55. Khan, H.; Shah, R.; Kumam, P.; Baleanu, D.; Arif, M. Laplace decomposition for solving nonlinear system of fractional order partial differential equations. *Adv. Differ. Equ.* **2020**, *2020*, 375. [[CrossRef](#)]
56. Mohyud-Din, S.T.; Noor, M.A.; Noor, K.I. Traveling wave solutions of seventh-order generalized KdV equations using he's polynomials. *Int. J. Nonlinear Sci. Num.* **2009**, *10*, 227–233. [[CrossRef](#)]
57. Liu, Y.Q. Approximate solutions of fractional nonlinear equations using homotopy perturbation transformation method. *Abstr. Appl. Anal.* **2012**, *2012*, 752869. [[CrossRef](#)]
58. Choi, J.; Kumar, D.; Singh, J.; Swroop, R. Analyttical techniques for system of time fractional nonlinear differential equations. *J. Korean Math. Soci.* **2017**, *54*, 1209–1229.